Cell Reports
Medicine

Article

A recombinant bovine adenoviral mucosal vaccine expressing mycobacterial antigen-85B generates robust protection against tuberculosis in mice

Graphical abstract

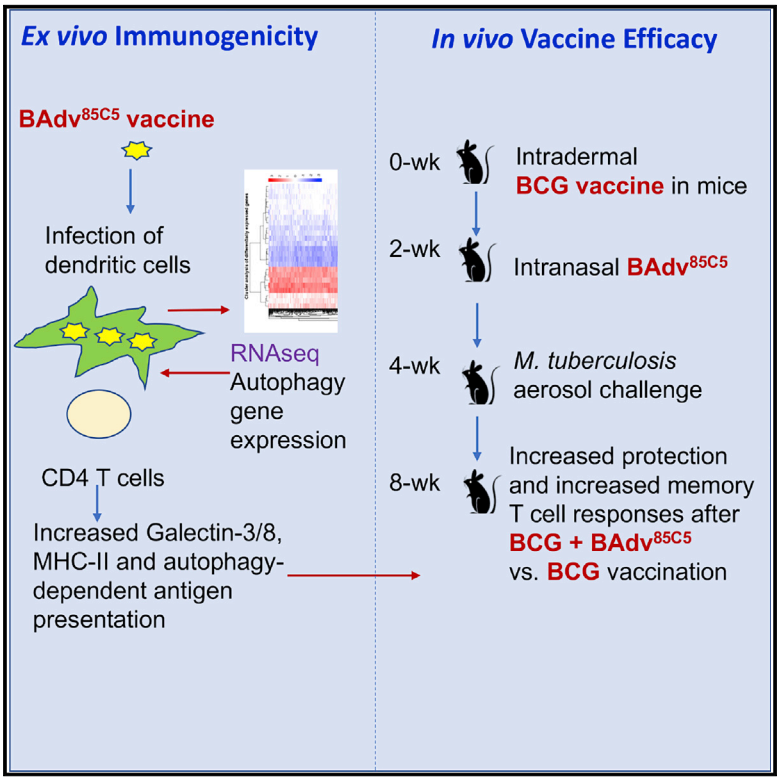

Highlights

- BCG-vaccinated infants need a booster for better protection against tuberculosis
- The BAdv^{85C5} vaccine increased protection in BCG-vaccinated mice against tuberculosis
- The BAdv^{85C5} vaccine increased antigen presentation and memory T cells responses
- Mucosal vaccination strengthens lung defense against tuberculosis

Authors

Arshad Khan, Ekramy E. Sayedahmed, Vipul K. Singh, ..., K. Jagannadha Sastry, Suresh K. Mittal, Chinnaswamy Jagannath

Correspondence

mittal@purdue.edu (S.K.M.), cjagannath@houstonmethodist.org (C.J.)

In brief

Khan et al. describe a bovine-adenovirus-based BAdv^{85C5} mucosal vaccine, which induced a galectin 3/8-dependent autophagy increasing antigen presentation in dendritic cells *ex vivo*. BAdv^{85C5} nasal booster in BCG-vaccinated mice enhanced the protection against tuberculosis and increased antigen-specific CD4 T cells and memory T cells.

Khan et al., 2021, Cell Reports Medicine *2*, 100372
August 17, 2021
https://doi.org/10.1016/j.xcrm.2021.100372

CellPress

Cell Reports Medicine

CellPress
OPEN ACCESS

Article

A recombinant bovine adenoviral mucosal vaccine expressing mycobacterial antigen-85B generates robust protection against tuberculosis in mice

Arshad Khan,[1,7] Ekramy E. Sayedahmed,[6,7] Vipul K. Singh,[1,7] Abhishek Mishra,[1,7] Stephanie Dorta-Estremera,[2] Sita Nookala,[2] David H. Canaday,[3] Min Chen,[4] Jin Wang,[5] K. Jagannadha Sastry,[2] Suresh K. Mittal,[6,*] and Chinnaswamy Jagannath[1,8,*]

[1]Department of Pathology and Genomic Medicine, Houston Methodist Academic Institute, Houston Methodist Research Institute & Weill Cornell Medical College, Houston, TX, USA
[2]Department of Thoracic Head and Neck Medical Oncology, MD Anderson Cancer Center, Houston, TX, USA
[3]Department of Medicine, Case Western Reserve University and Cleveland Veterans Affairs, Cleveland, OH, USA
[4]Department of Pathology and Immunology, Baylor College of Medicine, Houston, TX, USA
[5]Immunobiology and Transplant Science Center, Houston Methodist Research Institute, and Department of Surgery, Weill Cornell Medical College, Houston, TX, USA
[6]Department of Comparative Pathobiology and Purdue Institute of Inflammation, Immunology, and Infectious Disease, College of Veterinary Medicine, Purdue University, West Lafayette, IN, USA
[7]These authors contributed equally
[8]Lead contact
*Correspondence: mittal@purdue.edu (S.K.M.), cjagannath@houstonmethodist.org (C.J.)
https://doi.org/10.1016/j.xcrm.2021.100372

SUMMARY

Although the BCG vaccine offers partial protection, tuberculosis remains a leading cause of infectious disease death, killing ~1.5 million people annually. We developed mucosal vaccines expressing the autophagy-inducing peptide C5 and mycobacterial Ag85B-p25 epitope using replication-defective human adenovirus ($HAdv^{85C5}$) and bovine adenovirus ($BAdv^{85C5}$) vectors. $BAdv^{85C5}$-infected dendritic cells (DCs) expressed a robust transcriptome of genes regulating antigen processing compared to $HAdv^{85C5}$-infected DCs. $BAdv^{85C5}$-infected DCs showed enhanced galectin-3/8 and autophagy-dependent *in vitro* Ag85B-p25 epitope presentation to CD4 T cells. BCG-vaccinated mice were intranasally boosted using $HAdv^{85C5}$ or $BAdv^{85C5}$ followed by infection using aerosolized *Mycobacterium tuberculosis* (Mtb). $BAdv^{85C5}$ protected mice against tuberculosis both as a booster after BCG vaccine (>1.4-log_{10} reduction in Mtb lung burden) and as a single intranasal dose (>0.5-log_{10} reduction). Protection was associated with robust CD4 and CD8 effector (T_{EM}), central memory (T_{CM}), and $CD103^+/CD69^+$ lung-resident memory (T_{RM}) T cell expansion, revealing $BAdv^{85C5}$ as a promising mucosal vaccine for tuberculosis.

INTRODUCTION

Mycobacterium tuberculosis (Mtb) is a leading cause of mortality, with 8 million cases and ~1.5 million deaths each year. Bacillus Calmette-Guérin (BCG) is a widely used live-attenuated vaccine for the primary immunization of children worldwide. BCG protects mostly against extrapulmonary tuberculosis (TB), with variable protection against pulmonary disease ranging from 0% to 80%.[1]

BCG efficacy is influenced by several factors, including population genetics, pre-exposure to environmental mycobacteria, and its ability to induce efficient antigen presentation to T cells.[2] We demonstrated earlier that BCG sequesters within immature phagosomes of antigen-presenting cells (APCs) with poor delivery to lysosomes.[3,4] This sequestration results in the decreased presentation of the BCG-derived Ag85B-p25 epitope to CD4 T cells in mouse and human macrophages.[3,5] We also reported that rapamycin can induce autophagy in APCs to enhance the delivery of BCG to lysosomes, thereby increasing antigen presentation to CD4 T cells *in vitro*[5] and enhancing BCG efficacy.[6,7] We have described a second-generation recombinant BCG vaccine overexpressing Ag85B protein (BCG^{85B}) that induces autophagy in APCs and more effectively protects against TB relative to BCG.[5] Our more recently described third-generation BCG^{85BC5} vaccine expresses TLR2-activating and autophagy-inducing peptide C5 (AIP-C5) from Mtb CFP10 protein and is more effective than BCG^{85B} for the prevention of TB in mice.[8] These studies suggest that autophagy induction can boost BCG efficacy. An autophagy-inducing recombinant BCG vaccine is under assessment in human clinical trials.[9]

Although millions of children receive BCG vaccination at birth, a larger number remain susceptible to lung TB.[10] Accordingly, childhood TB remains common in many developing countries.

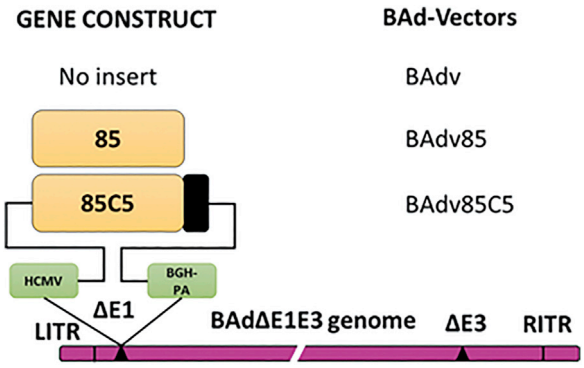

Figure 1. Diagrammatic representation of the gene cassette of the Ag85B-p25 epitope of *Mycobacterium tuberculosis* with or without the autophagy-inducing peptide C5 (AIP-C5) and the resultant BAdv vectors

The 2 peptides were separated by the AlaAlaAla linker. The gene cassette was under the control of the cytomegalovirus (CMV) promoter and the bovine growth hormone (BGH) polyadenylation (PA) signal. The drawings are not to scale. 85, Ag85B-p25 epitope; C5, AIP-C5; LTR & RTR, the left and right terminal repeats; ΔE1, deletion of the early region 1; ΔE3, deletion of the early region 3. qPCR validation of Ag85B epitope and C5 epitope and the gene cassette for HAdv^{85C5} vectors and vaccines are shown in Figures S1A and S1B respectively.

Because the main portal of entry for Mtb is respiratory, strengthening the neonatal lung immune response is a rational approach to prevent both pulmonary and extrapulmonary TB. Multiple studies suggest that viral vector-based vaccine platforms for Mtb are excellent in inducing both systemic and mucosal immunity.[11–20] However, respiratory mucosal booster vaccines following BCG immunization may not offer adequate protection from TB in neonates owing to the defective expansion of resident memory T cells (T_{RM}).[21] Recent evidence indicates that the neonatal immune system is functional but physiologically immature and requires vaccine adjuvants to elicit robust T helper (T_H) cytokine responses in APCs.[22,23] The relevance of an immature neonatal immune system in the context of disease is underscored by the requirement for childhood vaccine boosters for diptheria and tetanus toxoids, pertussis vaccine (DTP), and measles-mumps-rubella (MMR) vaccine. The immature neonatal immune system and the intrinsic defects of the BCG vaccine in APCs combined may explain the occurrence of lung TB and increased Mtb dissemination in neonates despite BCG vaccination.

Because BCG vaccination is continuing and there is an important need to protect children using safer vaccines, we sought to design an efficient vaccine platform capable of enhanced antigen presentation through autophagy. We have developed a bovine adenovirus (BAdv)-based TB vaccine expressing the immunodominant mycobacterial Ag85B-p25 epitope along with AIP-C5. Importantly, pre-existing adenovirus (Adv) antibodies do not interfere with the immunogenicity of BAdv vector-based vaccines.[24–26] Our engineered mucosal vaccine augmented the ability of APCs to process and present the Ag85B-p25 epitope to CD4 T cells. Our nasal vaccine protected mice following aerosolized challenge with Mtb, both as a booster after BCG vaccine and alone. Finally, we observed a marked expansion of CD4 and CD8 effector (T_{EM}), central memory (T_{CM}), and CD103$^+$/CD69$^+$ T_{RM} T cells in the lungs of vaccinated mice, suggesting that the vaccine protects mice from TB by inducing a robust pulmonary immune response.

RESULTS

Characterization of BAdv or human Adv (HAdv)-based vectors expressing the Mtb Ag85B-p25 epitope with or without AIP-C5

Adv vector-based vaccines elicit both humoral and cell-mediated immune (CMI) responses[26,27] due to the adjuvant-like effect of Adv vectors by activating the innate immune system through both Toll-like receptor (TLR)-dependent and TLR-independent pathways.[25,28] Influenza is one of the significant respiratory diseases in humans, animals, and birds. Adv vector-based influenza vaccines have conferred protective efficacy in both animal models[29–31] and clinical trials in humans.[14,32–35]

We expressed the Mtb Ag85B-p25 epitope with or without AIP-C5 in the replication-defective BAdv or HAdv vector system.[36] The Mtb Ag85B-p25 epitope (85) or 85 + AIP-C5 (85C5) gene cassette was under the control of the immediate early cytomegalovirus (CMV) promoter and bovine growth hormone (BGH) polyadenylation (PA) signal. The generated vectors BAdv^{85} (expressing 85), BAdv^{85C5} (expressing 85C5), HAdv^{85} (expressing 85), or HAdv^{85C5} (expressing 85C5) (Figure 1) were assessed for gene cassette expression using sequencing and RT-PCR (Figure S1A). HAdv constructs are shown in Figure S1B and were used in several experiments for comparison.

Replication-defective BAdv^{85C5} vaccine efficiently infects immature mouse dendritic cells (DCs) and induces a robust transcriptome

To characterize the virus-induced transcriptome, bone marrow-derived CD11c$^+$ immature DCs from wild-type (WT)-C57BL/6 mice and autophagy-deficient *ATG7*KO-DC mice[37] were infected with BAdv^{85C5}, BAdv vector, HAdv^{85C5}, or HAdv vector followed by RNA sequencing (RNA-seq) analysis (Novogene). Figure 2A illustrates the heatmap of differentially expressed genes (DEGs) (n = 2) of BAdv- and HAdv-derived vaccine or vector-infected WT-DCs and *ATG7*KO-DCs. ClusterProfiler analysis (Novogene) showed a relative enrichment of multiple genes in BAdv^{85C5}- versus HAdv^{85C5}-infected WT-DCs. KEGG (Kyoto Encyclopedia of Genes and Genomes) and Gene Ontology (GO; cellular components [CC] and biological processes [BP]) profiles are illustrated in Figures 2B–2E. Intriguingly, heatmaps of transcripts derived from RNA-seq expressed as FPKMs (fragments per kilobase per million mapped reads; n = 2) show that BAdv^{85C5} upregulated the expression of gene clusters involved in antigen processing and endosome sorting to lysosomes. For example, cathepsins (*CTSA*, *CTSB*, *CTSK*, *CTSS*, *CTSL*, and *CTSZ*) were enriched in BAdv^{85C5}-infected DCs compared to HAdv^{85C5} (Figures 2F and 2G) (see also Figure S2). CTSs proteolytically cleave antigens into peptides and help their loading onto the major histocompatibility complex class II (MHC class II), which are in turn, exported to the plasma membrane for activation of CD4 T cells. Furthermore, BAdv^{85C5} upregulated the

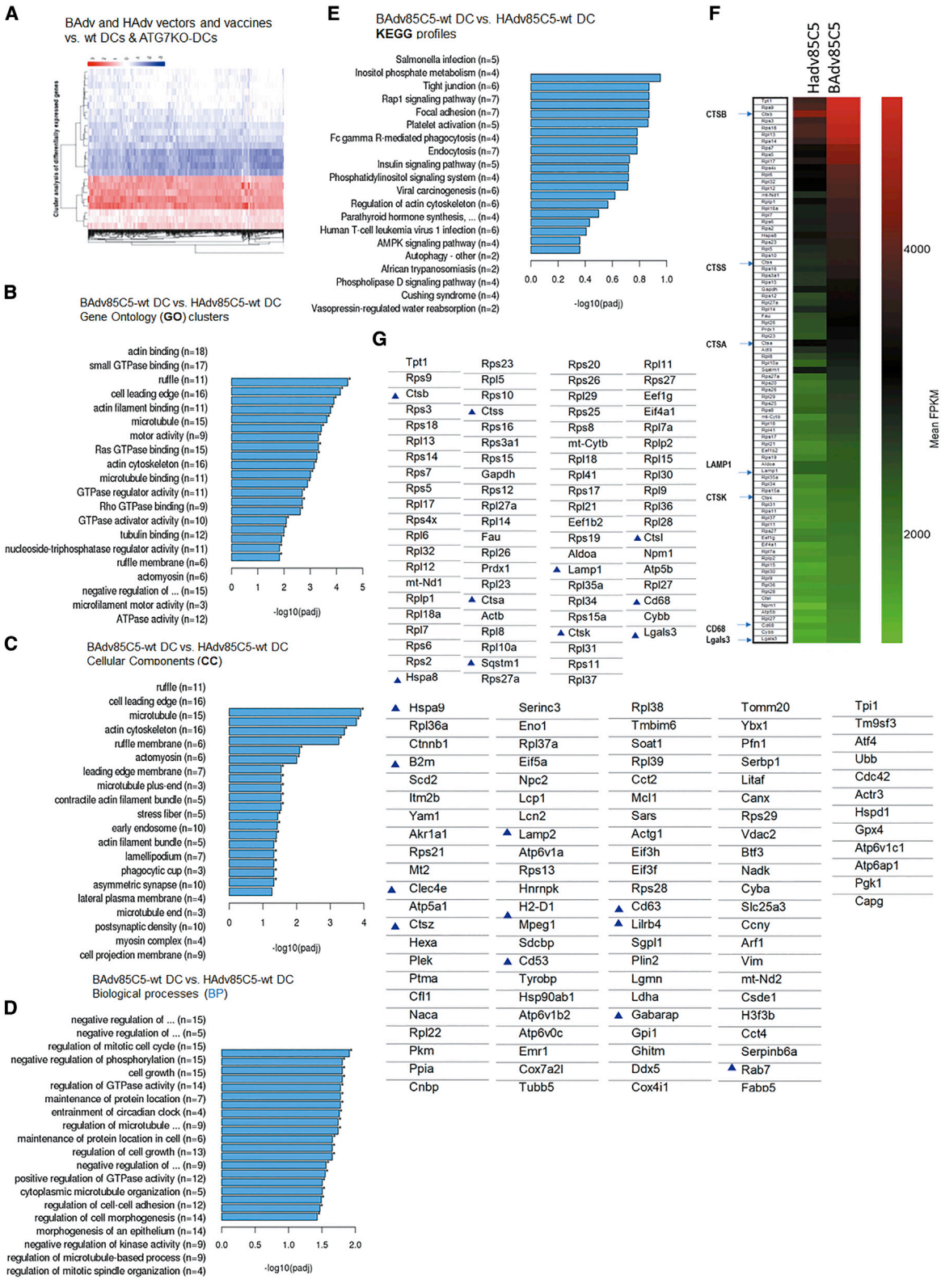

(legend on next page)

genes of the MHC pathway (*H2-D1, B2m*), and *LAMP1*, *LAMP2*, *Hspa8*, *Hspa9*, *CD68 (LAMP4)*, and galectin3 (Gal3; also known as *Lgals-3*), which participate during the sorting of antigens and pathogens into the lysosomes.[38–40] Transcripts for *Lgals-8* were also found to be enriched BAdv^{85C5}-infected DCs (mean FPKMs 510 ± 15; BAdv^{85C5}750 ± 55 versus HAdv^{85C5}, $p < 0.001$; data not shown). Finally, *Gabarap* (LC3 family), *SQSTM1*, and *Rab7* were upregulated in BAdv^{85C5}-infected DCs and are key players during autophagolysosome fusion.[41,42] Many of these genes were also selectively upregulated by BAdv^{85C5}-infected WT-DCs compared to *ATG7*KO-DCs (Figure S3), suggesting that BAdv^{85C5}-upregulated genes are associated with autophagy. qPCR validation of the genes involved during antigen sorting and processing is shown in Figure S4 and is discussed in the context of vaccine-induced immunogenicity below.

Replication-defective BAdv^{85C5} vaccine is rapidly internalized by DCs and localizes to autophagolysosomal compartments

DCs are essential for vaccine-induced immune responses in both mice and humans.[43] Earlier studies indicated that Cy3-fluorescent labeled Adv retain >98% infectivity.[44] Therefore, we used Cy3-labeled BAdv^{85C5} or BAdv vector for the infection of mouse CD11c^{+} immature DCs followed by confocal microscopy. Since Adv can interact with the autophagy pathway and microtubule-associated light chain 3 (LC3) is a known marker of autophagosomes, LC3 was used as a marker for the virus containing endosomes.[45] Cy3-BAdv^{85C5} and Cy3-BAdv vectors were rapidly internalized, and Figure 3 illustrates their uptake; both were found distributed between the cytosol and nucleus after a 4-h infection cycle, similar to a previous report.[46] Endosomes colocalizing with the LC3 marker were quantitated, indicating an increased labeling of Cy3-BAdv^{85C5} endosomes compared to those containing Cy3-BAdv vector (Figure 3A). Similarly, lysosome-associated membrane protein-1 (LAMP1) labeling was higher, suggesting that Cy3-BAdv^{85C5} localizes more in autophagolysosomes than the vector (Figure 3B). Previous studies indicate that autophagy plays a role during the translocation of Adv capsids from the endosome to the nuclear pore complex, and during this process, lectin-like intracellular receptors Gal3 and Gal8 (*Lgals-3/8*) are associated with the vesicular transport of Adv.[47,48] BAdv^{85C5}-infected DCs showed a stronger enrichment of both *Lgals-3* and *Lgals-8* (Figures 3C and 3D). Isotype control is shown in Figure S5. It is pertinent to recall here that HAdv infects immature mouse DCs less effectively than a HAdv vector engineered to target DCs.[49] In contrast, DCs efficiently internalized both Cy3-BAdv^{85C5} and Cy3-BAdv vectors. Whereas HAdv^{85C5} and BAdv^{85C5} are associated with the autophagy pathways in DCs, BAdv^{85C5} shows an enhanced expression of genes correlating with endosome traffic.

Replication-defective BAdv^{85C5} vaccine enhances autophagy-dependent and -independent antigen presentation in mouse DCs and human macrophages

Previous studies show that HAdv vectors expressing mycobacterial antigens protect mice and macaques against TB variably, although human studies have not been encouraging.[13,19,50] Because BAdv^{85C5} induced robust gene expression in DCs, we sought to determine whether it increases the immunogenicity of DCs compared to HAdv^{85C5}.

A major function of vaccine-ingested DCs is an efficient antigen processing and activation of CD4 and CD8 T cells through the MHC class II and the MHC class I pathway, respectively. Whereas vaccines degraded in lysosomes are routed to the MHC class II pathway, proteasome-digested peptides of vaccines are routed through MHC class I. We demonstrated earlier that autophagy can increase the MHC class II-dependent presentation of mycobacterial Ag85B,[5] whereas autophagy was also reported to increase the MHC class I-dependent presentation of antigens in APCs.[51] To define DC-mediated antigen-processing mechanisms, we used a well-characterized *ex vivo* assay wherein BCG- or Mtb-infected APCs rapidly present an Ag85B-derived p25 epitope to BB7 CD4 T cells *ex vivo* in the presence or absence of autophagy.[3,52–55]

Autophagy begins with an intracellular membrane vesicle nucleation, vesicle elongation, and autophagophore formation, which encloses pathogens in an autophagosome. The latter fuse with the lysosomes, which in turn, degrade pathogens generating antigenic peptides through CTS proteases. This process, also known as macroautophagy, involves several autophagy-regulating genes (*ATG*s), of which *ATG7* and *ATG5* are key genes, although alternative pathways exist.[56] To determine whether autophagy plays a role during virus vaccine-induced antigen presentation, we infected WT-DCs and *ATG7*KO-DCs with BAdv^{85C5} or HAdv^{85C5} followed by antigen presentation. *ATG7* deficiency in DCs led to a significant reduction in antigen presentation after infection with either BAdv^{85C5} or HAdv^{85C5} (Figure 4A). Supporting these data, WT-DCs and *ATG7*KO-DCs infected with BAdv^{85C5} showed striking differences in gene expression, indicating that autophagy is important during BAdv^{85C5} vaccine antigen processing (Figure S3). BAdv^{85C5} also showed upregulated antigen presentation in macrophages comparable to HAdv^{85C5} (Figure 4B) and enhanced gene expression compared to HAdv^{85C5} vaccine (Figure S6).

Because the BAdv^{85C5} vaccine platform is being developed for human neonates following BCG vaccination, we also treated human CD14^{+} macrophages with an autophagy inhibitor,

Figure 2. Replication-defective BAdv^{85C5} vaccine induces a robust transcriptome in mouse DCs compared to HAdv^{85C5} vaccine

(A) Heatmaps of differentially expressed genes (DEGs) among DCs infected with BAdv- or HAdv-derived vaccines or vectors are shown (n = 2). Additional DEGs are shown in Figures S2, S3 and S6.

(B–E) Gene expression analysis using ClusterProfiler (Novogene) indicated as KEGG (Kyoto Encyclopedia of Genes and Genomes) profiles followed by Gene Ontology (GO), cellular components (CC), and biological processes (BP).

(F) Heatmaps of transcripts derived from RNA-seq expressed as FPKMs (fragments per kilobase per million mapped reads; n = 2); BAdv^{85C5} vaccine upregulated genes involved in antigen processing are reproduced to the left and enriched genes are highlighted in blue ($p < 0.0001$, n = 2) (see also Figure S2).

(G) Partial listing of DEGs are shown and those associated with antigen processing or endosome sorting are highlighted.

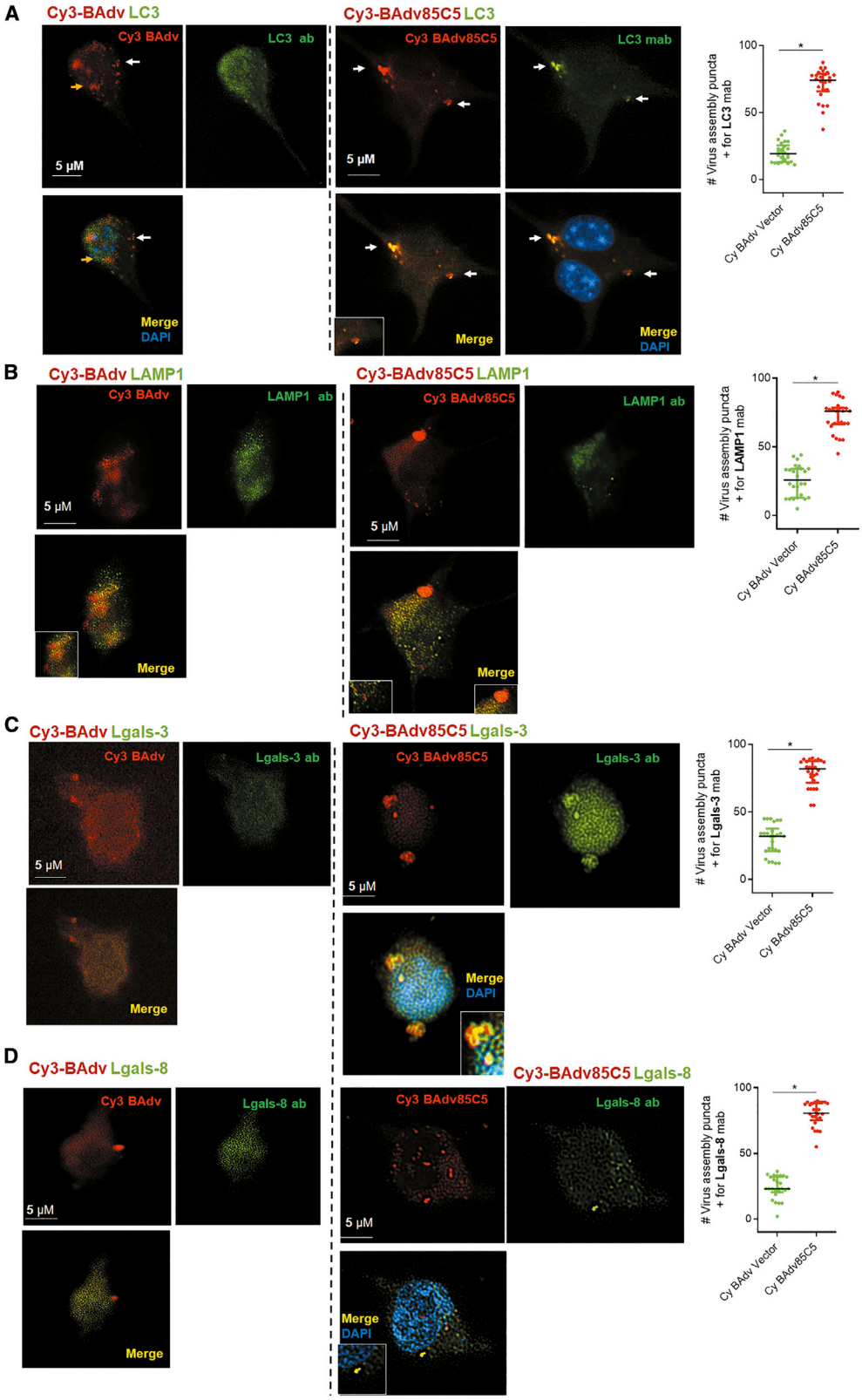

(legend on next page)

3-methyladenine (50 μM), followed by infection with BAdv^{85C5} or HAdv^{85C5}. Autophagy blockade reduced antigen presentation by both BAdv^{85C5} and HAdv^{85C5} in human CD14^{+} macrophages (Figures 4C and 4D). However, BAdv^{85C5} induced an elevated and sustained increase in antigen presentation in human CD14^{+} macrophages compared to HAdv^{85C5} (Figure 4E). Previously, we found that autophagy-mediated delivery of mycobacteria to lysosomes results in their degradation and reduced viability.[5] Mouse CD14^{+} macrophages were infected with vectors or vaccines followed by infection with Mtb and growth assay. BAdv^{85C5} showed a better ability to reduce the viability of intracellular Mtb than HAdv^{85C5} or vectors (Figures 4F and 4G). These data indicate that BAdv^{85C5} induces a robust autophagy-mediated antigen presentation to CD4 T cells in mouse DCs, mouse macrophages, and human macrophages.

Replication-defective BAdv^{85C5} vaccine induces expression of galectins and CTSs to enhance antigen presentation in DCs

Previous studies show that autophagy plays a role during the translocation of Adv capsids from the endosome to the nuclear pore complex.[45] During this process, galectins, specifically, Gal1 (*Lgals-1*) and Gal3 (*Lgals-3*), were found to be associated with the vesicular transport of Adv;[45] however, HAdv5 infection of A549 epithelial cells strongly downregulated Gal3 (*Lgals-3*) expression.[57] Transcriptomic studies show that *Lgals-3* (Figure 2) and *Lgals-8* (not shown; below the level of FPMKs indicated) transcripts were upregulated in BAdv^{85C5}-infected DCs. qPCR validation showed that BAdv^{85C5}-induced increased mRNA transcripts for *Lgals-3* and *Lgals-8* relative to HAdv^{85C5}-infected DCs (Figure 5A). Interestingly, western blots indicated that *Lgals-3* was uniformly induced in DCs by both vectors and vaccines, while *Lgals-8* was induced more strongly in BAdv^{85C5}-infected DCs (Figure 5B). qPCR and western blot analysis of BAdv^{85C5}- and HAdv^{85C5}-infected DCs also showed that the enrichment of other autophagy-related genes, including *Gabarap* (LC3 family); *SQSTM1* (a known substrate of autophagy), and *Rab7* (a small GTPase), are essential for the fusion of autophagosomes to lysosomes.[58]

Because *Lgals-3* binds the tripartite containing motif protein-16 (TRIM16) to activate autophagy through *ATG*1/ulk1, we hypothesized that BAdv^{85C5} may induce autophagy through a *Lgals-3*- and/or *Lgals-8*-dependent mechanism.[59–61] We reported that autophagy enhances the ability of APCs (macrophages; and DCs) to process and present a mycobacterial antigen to CD4 T cells[5]. Therefore, we performed small interfering RNA (siRNA) knockdown of galectins in APCs. BAdv^{85C5}- or HAdv^{85C5}-infected DCs or macrophages were subjected to siRNA versus *Lgal-3* and *Lgals-8* or siRNA versus *Lgals*-3, respectively. Galectin knockdown reduced antigen presentation by both BAdv^{85C5}- and HAdv^{85C5}-infected DCs or macrophages (Figures 5C and 5D). We note here that WT HAdv modulates autophagy through a Nedd4.2 pathway, reducing antigen presentation.[48] We suggest that BAdv^{85C5} may augment autophagy and antigen presentation through the induction of *Lgals-3*; however, additional studies are required to determine whether *Lgals-8* synergizes to activate autophagy.[62]

DCs degrade mycobacteria in their lysosomes using proteases such as CTSs, lipases, and glycosidases. We demonstrated earlier that CTSD cleaves Ag85B in mouse macrophages to generate the p25 epitope, which is then rapidly presented to CD4 T cells *in vitro*.[3] CTSs not only digest proteins but also help to load peptides into the groove of MHC class II, and CTSS and CTSL play a pivotal role.[63,64]

DC transcriptome studies indicated that BAdv^{85C5} enhanced the expression of multiple CTSs (Figure 2F). Figure 5E shows qPCR validation of increased CTS expression by BAdv^{85C5}-infected DCs compared to HAdv^{85C5}-infected DCs. During antigen processing and presentation, CTSB, CTSS, and CTSL seem to play major roles compared to CTSA, CTSK, and CTSZ.[64] Western blot studies confirmed a better expression of CTSB, CTSS, and CTSL by BAdv^{85C5}-infected DCs (Figure 5F). To determine whether CTSs mediate the processing of virus-encoded antigens, WT-DCs and *ATG7*KO-DCs were pharmacologically blocked using pan-specific CTS inhibitors E64 and *N*-acetyl-L-leucyl-L-leucyl-L-methional (NALLM), and the CTSL inhibitor calpeptin, followed by infection with BAdv^{85C5} or HAdv^{85C5} and antigen presentation. All three CTS inhibitors reduced antigen presentation in WT-DCs, but only the pan-inhibitor E64 had an inhibitory effect on BAdv^{85C5}- or HAdv^{85C5}-infected *ATG7*KO-DCs (Figure 5G). These data indicate that BAdv^{85C5} increases the immunogenicity of DCs through CTS-dependent antigen processing and presentation.

BAdv^{85C5} mucosal vaccine protects mice against aerosolized Mtb independently and as a BCG booster

To determine whether BAdv^{85C5} enhances immunogenicity *in vivo*, we intranasally inoculated age- and sex-matched inbred C57BL/8 mice, which show a "developing immune system" akin to the neonatal immune system,[65] with vaccines or empty vectors. At 3 days post-inoculation, we euthanized the animals and analyzed bronchoalveolar lavage (BAL) cells and lung tissues using qPCR. BAdv^{85C5} markedly enhanced mRNA transcripts for a panel of genes associated with antigen processing and presentation compared to HAdv^{85C5} (Figures 6A and S4).

Figure 3. Replication-defective BAdv^{85C5} vaccine is rapidly internalized by mouse DCs

CD11c^{+} DCs purified from bone marrow of WT-C57BL/6 mice were infected with the Cy3-labeled BAdv^{85C5} vaccine or control vector (10^{7} PFU/10^{6} DCs), followed by antibody staining for intracellular localization using confocal microscopy at 4 h post-infection. Cy3-BAdv vector or Cy3-BAdv^{85C5} vaccine-infected DCs were incubated for a 4-h infection, followed by fixation and staining using specific antibodies to (A) microtubule associate light chain 3 (LC3) autophagosome marker, (B) lysosome associated membrane protein-1 (LAMP1), (C) galectin3 (*Lgals-3*), and (D) *Lgals-8* followed anti-immunoglobulin G (IgG) Alexa Fluor 488 and DAPI nuclear stain. Panels show Cy3 (red), Alexa Fluor 488 (green), and merged images with or without DAPI nuclear stain. Colocalization (inset) analyzed using confocal microscopy and Nikon N90 microscope with MetaView software. Cytosolic (white arrow) and nuclear localization (yellow arrow) of Cy3-labeled vector or vaccines are indicated. Bar graphs to the right show percentage of virus-containing endosomes colocalizing with antibodies calculated per DC and averaged for 20 DCs in triplicates per experiments done twice. *$p < 0.01$ t test. Isotype stains are shown in Figure S5.

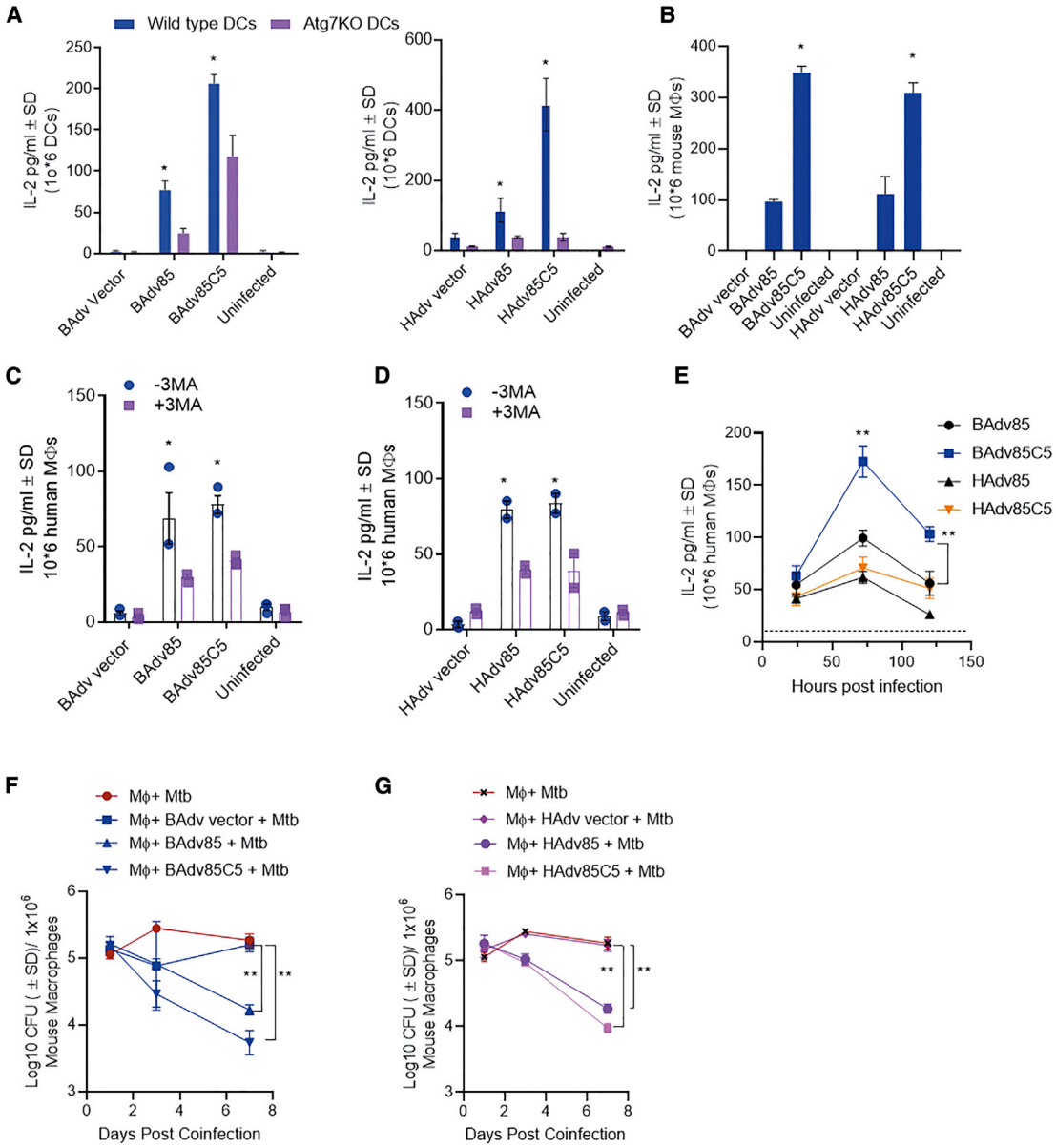

Figure 4. Replication-defective BAdv^{85C5} vaccine enhances autophagy-dependent and -independent antigen presentation in mouse DCs and human macrophages

(A) WT-C57BL/6- or *ATG7*KO-C57BL/6-derived DCs were infected with vaccines or control vectors (10^7 plaque-forming units [PFUs]/10^6 DCs) followed by overlay using BB7 CD4 T cells specific for the Ag85B-p25 epitope in the context of MHC class II. IL-2 in supernatants at 18 h post-infection was determined using sandwich ELISA.

(B) Antigen presentation in vaccine- or vector-infected mouse macrophages (10^7 PFU/10^6 macrophages) is shown.

(C and D) Human peripheral blood mononuclear cell (PBMC)-derived CD14$^+$ macrophages were infected with vaccines or control vectors followed by an overlay with F9A6 T cells specific for an Ag85B epitope in the context of human leukocyte antigen-DR1 (HLA-DR1) for antigen presentation. Macrophages were untreated or treated with 3-methyladenine (50 μM) before infection to inhibit autophagy.

(E) Time-dependent antigen presentation by human macrophages infected with BAdv- or HAdv-derived vaccines. Horizontal line shows IL-2 levels of T cells incubated over naive macrophages.

(F and G) CD14$^+$ mouse bone marrow-derived macrophages were infected with 10^6 PFUs of vectors and vaccines indicated for 4 h, followed by co-infection with Mtb (Erdman strain; MOI = 1), washing, and incubation. Macrophage lysates were plated for CFU counts at indicated time points. For all of the panels, 1 of 2–3 separate experiments shown.

*$p < 0.01$; **$p < 0.009$ 1-way ANOVA with Tukey's test.

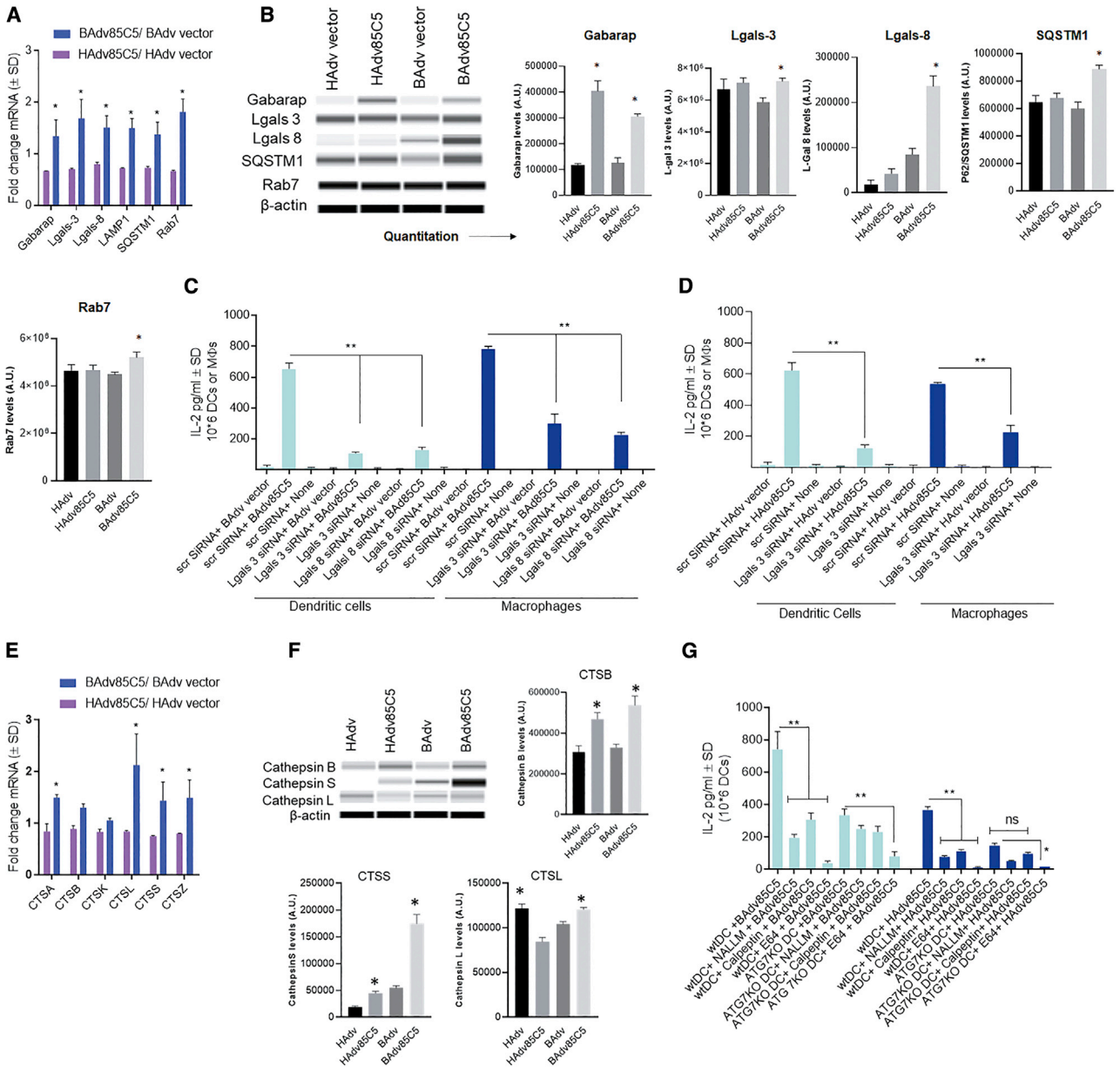

Figure 5. Replication-defective BAdv^{85C5} vaccine enhances galectin and cathepsin-dependent antigen presentation in mouse DCs and human macrophages

C57BL/6 mouse-derived DCs were infected with vaccines or control vectors, washed, and processed.

(A) At 18 h post-infection, lysates collected in Trizol were used for qPCR using primers (Method details) for endosome trafficking genes enriched during transcriptomics (Figure 2) (*≥1.4-fold increase in mRNA expression, n = 2, 2 experiments).

(B) At 18 h post-infection, lysates collected in anti-protease buffer analyzed using specific antibodies and Wes Simple blot protocol (Method details). Densitometry panels shown.

(C and D) DCs and macrophages were subjected to siRNA versus *Lgals-3* and *Lgals-8* or scrambled controls and at 18 h, infected using vaccines or vectors for 4 h. Washed DCs were overlaid using BB7 CD4 T cells, and 18 h later, supernatants assayed for IL-2 using sandwich ELISA (triplicate wells of DCs per group and 2 independent experiments).

(E) Lysates collected at 18 h post-infection were used for qPCR using primers (Method details) for cathepsins enriched during transcriptomics (Figure 2) (*≥1.4-fold increase in mRNA expression, n = 2, 2 experiments).

(F) Lysates collected at 18 h post-infection were analyzed using specific antibodies and Wes Simple blot protocol (Method details).

(G) WT-DCs or *ATG7*KO-DCs DCs were left untreated or treated with cathepsin inhibitors as indicated, followed by vaccine or vector infection and antigen presentation. NALLM, *N*-acetyl-L-leucyl-L-leucyl-L-methional; calpeptin; E64, each at 30 μM; triplicate wells of DCs per group and 2 independent experiments. *$p < 0.01$, **$p < 0.006$, 1-way ANOVA with Tukey's post-test.

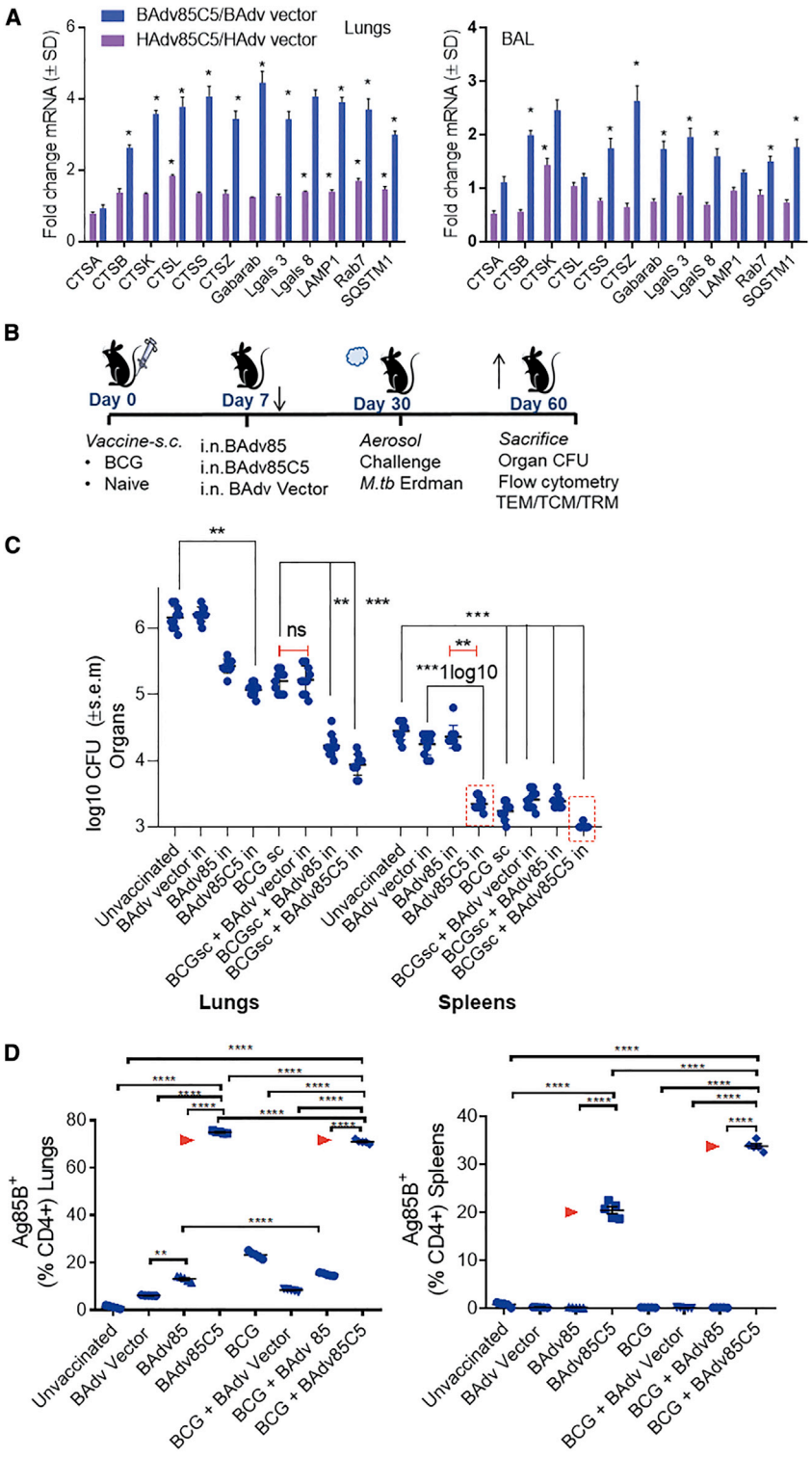

Figure 6. BAdv^{85C5} mucosal vaccine protects mice against aerosolized Mtb either alone or as a booster following BCG vaccine

(A) Female or male C57BL/6 mice, 4–6 weeks old, were nasally instilled using 1 dose each of vaccines or vectors at 10^7 PFUs. After 3 days, mice were sacrificed and bronchoalveolar lavage (BAL) cells and lung tissue suspended in Trizol and subjected to qPCR for gene expression (*≥1.4-fold increase in mRNA expression, n = 2, 2 independent experiments).

(B) Female or male C57BL/6 mice, 4–6 weeks old, were mock-inoculated or vaccinated subcutaneously with BCG. At 7 days post-immunization, animals received a single intranasal booster vaccination with 10^7 PFUs of BAdv,[66] BAdv^{85C5}, or BAdv vector control. Three weeks later, mice were aerosol challenged with Mtb ~100 CFU of Erdman using a Glas-Col inhalation apparatus. Four weeks later, mice were sacrificed for Mtb counts, followed by analysis of the lungs and spleen for T cell profiles (Figure 7).

(C) BAdv^{85C5} reduces the lungs and spleen burden of Mtb (**p < 0.007, ***p < 0.004; 2-way ANOVA with Dunnett's post-test; n = 10, 5 mice per group each from 2 independent experiments plotted).

(D) Flow cytometry data presented for 1 of 2 similar experiments integrated in (C). Lungs and spleen of mice collected post-Mtb challenge were stained using Ag85-p25 epitope-specific MHC class II tetramer (NIH tetramer core facility, Emory University) and analyzed using flow cytometry (n = 3 from the same group of mice, B and C; ****p < 0.001; ordinary 1-way ANOVA). Arrowheads indicate BAdv^{85C5} induced T cell expansion.

We mock-inoculated or subcutaneously vaccinated mice with BCG and administered a single intranasal booster vaccination with BAdv^{85}, BAdv^{85C5}, or BAdv vector control 7 days post-immunization (Figure 6B). After 3 weeks, we administered an aerosolized Mtb Erdman challenge. At 4 weeks post-challenge, we euthanized the mice and collected lungs and spleen for Mtb bacterial counts and T cell profiling. Compared to vector, BAdv^{85C5} induced robust protection against Mtb as a booster following primary BCG vaccination, reducing lung Mtb burden by >1.4 $\log_{10}$ and spleen load by ~0.8 $\log_{10}$ (Figure 6C). BAdv^{85} generated a comparable decrease in Mtb colony-forming units (CFUs) in the lungs and spleen. However, only the autophagy-inducing BAdv^{85C5} dramatically reduced spleen CFUs (≥1.0 $\log_{10}$) as an intranasal treatment alone. To confirm the specificity of the Ag85B-p25 immunogenic epitope, we stained lung- and spleen-derived T cells with an Ag85B-specific tetramer. Flow cytometry analysis showed that BAdv^{85C5} induced a robust expansion of Ag85B-p25-specific CD4 T cells in the lungs and spleen, consistent with reports that the Ag85B-p25 epitope protects mice against TB (Figure 6D).[8,18] Finally, co-expression of the AIP-C5 peptide in BAdv^{85C5} led to a robust tetramer-positive CD4 T cell

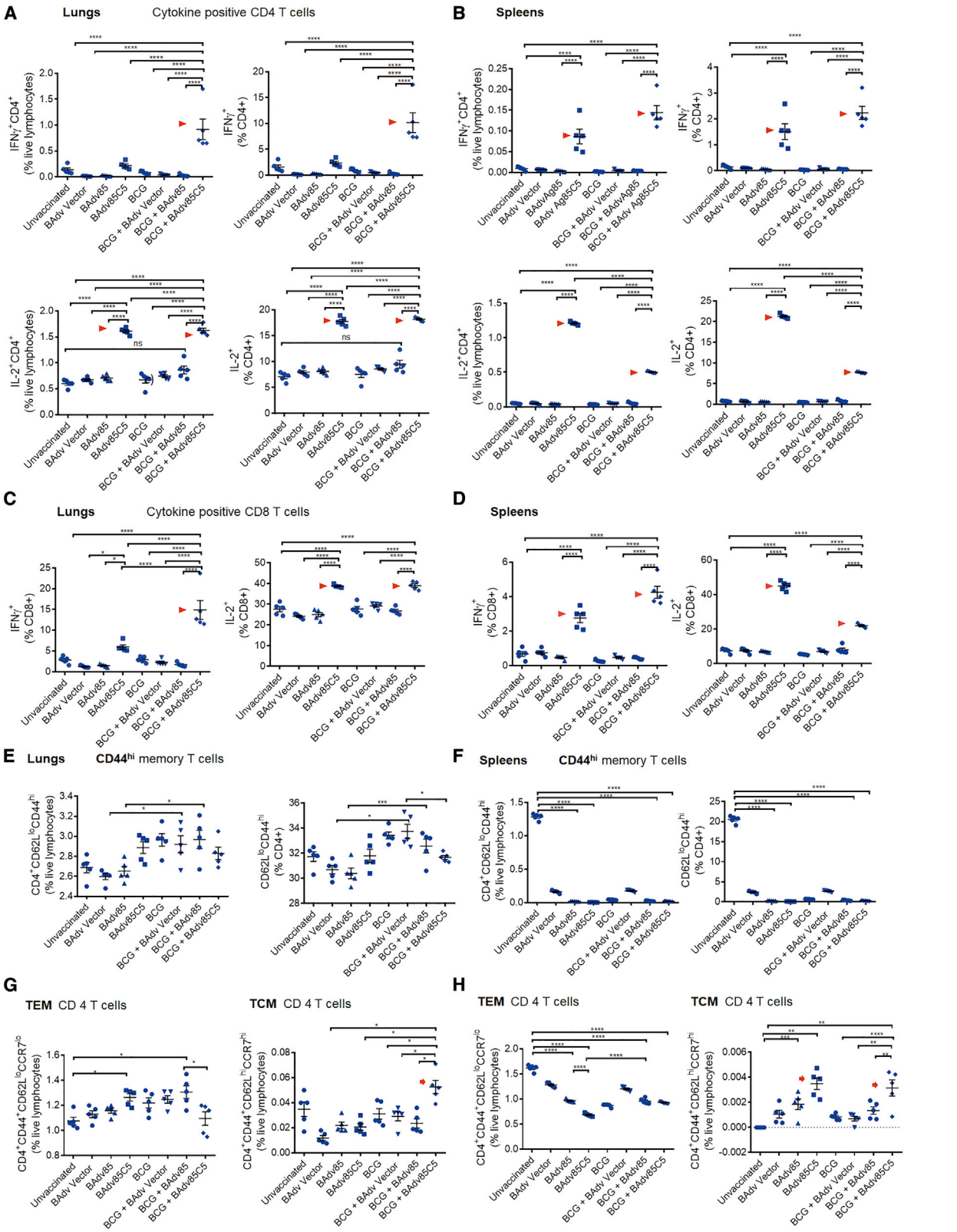

(legend on next page)

response in the lungs compared to the BAdv^{85} vaccine (Figure 6D).

We note here that BAdv^{85C5} induced a dramatic expansion of tetramer-positive CD4 T cells compared to mice vaccinated using recombinant BCG^{85C5} and Mtb-challenged mice in our previous study.[8] This augmentation can be explained by the immunodominance of the p25 epitope and its ability to activate naive T cells toward the Th1 pathway.[67] Notably, unlike BCG^{85C5} given intradermally in our recent study, BAdv^{85C5} was given nasally, enabling a robust activation of lung APCs to induce tetramer-positive cells. Supporting this observation, co-expression of the AIP-C5 peptide in BAdv^{85C5} led to a robust tetramer-positive CD4 T cell response in the lungs compared to BAdv^{85} vaccine (Figure 6D). These data suggest that BAdv^{85C5} expressing one major antigenic epitope of Mtb (Ag85B) can serve as a robust mucosal vaccine, even when administered as a single dose.

A BAdv^{85C5} booster induces cytokine-positive T cells, T_{EM} cells, and T_{CM} cells in BCG-vaccinated mice

Because T_H1 immunity-mediating T cell-secreted cytokines such as interferon-γ (IFN-γ) and interleukin-2 (IL-2) play a major defensive role against TB in mice and humans,[68] we investigated whether BAdv^{85}, BAdv^{85C5}, or BAdv vectors affected these cytokines when administered as a single dose or as a booster. BAdv^{85C5} vaccine significantly enhanced IFN-γ- and IL-2-expressing CD4 and CD8 T cells compared to either BAdv^{85} or BAdv vector (Figures 7A–7D). Importantly, BAdv^{85C5} induced an expansion of IFN-γ$^+$ and IL-2$^+$ T cells in lung and spleen when given as an intranasal vaccine, suggesting that irrespective of BCG vaccination, it can elicit immune responses and adults can also be nasally vaccinated against TB.

Respiratory infections induce a T_{EM} cell response, which enables an immediate containment of infection, followed by their transition into a long-lasting T_{CM} cell response. In many viral infection models and LCMV (lymphocytic choriomeningitis virus) infection of mice, T_{CM} cells mediate long-term immunity.[69–71] Since the lungs are not lymphoid organs, T_{EM} and T_{CM} are thought to arise in the lymph nodes and home back to the lungs for the containment of infection recruited by the chemokines secreted from the Mtb-infected macrophages. For example, chemokine receptors CCR2, CXCR5, CCR5, and CXCR6 enhance lung infiltration with T_H1-type immune cells, and CCR2-deficient mice are highly susceptible to TB.[72,73] Figures 7E–7H demonstrate that both BAdv85 and BAdv^{85C5} induced an expansion of T_{EM} cells in the lungs and spleens of the BCG-vaccinated mice, although only BAdv^{85C5} induced a significant T_{CM} response. BCG induces a robust T_{EM} response, but a reduced T_{CM} response in mice.[74] Therefore, we propose that using BAdv^{85C5} as a booster in BCG-vaccinated mice can augment long-lived memory T cells.

BAdv^{85C5} booster induces robust lung-resident T_{RM} cell expansion in BCG-vaccinated mice after Mtb challenge

T_{RM} cells are thought to play a major role in defending against airborne infections,[75,76] and attenuated T_{RM} cell expansion after infection has been observed in both human infants and neonatal mice.[21] The use of an adjuvant with a peptide vaccine has been shown to augment lung T_{RM} responses.[77] Thus, we assessed whether BAdv^{85C5} could induce a more robust T_{RM} response in the lungs of BCG-vaccinated and -boosted mice before and after challenge with Mtb. BAdv^{85C5} augmented the expansion of T_{RM} cells in both lung and spleen in the BCG-boosted, and Mtb-challenged groups (Figure S7). As even single doses of BAdv85 and BAdv^{85C5} induced T_{RM} cell expansion, they are promising candidates to protect lungs against TB.

DISCUSSION

This study presents an alternative BAdv vaccine platform approach to HAdv-based TB vaccines, which have shown promise in mouse and macaque models,[13,19] but not in human studies.[50] We have previously demonstrated that BAdv vector-based vaccines are effective in the presence of exceptionally high levels of preexisting HAdv vector immunity[24]; thus, preexisting HAdv vector immunity should not affect vaccine efficacy. Furthermore, BAdv3 internalization is independent of HAdv5 receptors (Coxsackievirus-Adv receptor [CAR] and αvβ3 or αvβ5 integrin),[78] and instead uses α(2,3)-linked as well as α (2,6)-linked sialic acid-containing proteins as major receptors.[79] Preexisting HAdv-neutralizing antibodies in humans do not cross-neutralize BAdv3,[80] and HAdv-specific immune response does not affect BAdv.[81] Notably, unlike HAdv5, BAdv3 is a strong inducer of TLR4 and does not deplete Kupffer cells of the liver.[25] Our previous biodistribution study using a BAdv3 vector in mice showed that BAdv3 efficiently transduces the heart, kidney, lung, liver, and spleen, and persists longer than HAdv5, particularly in the heart, kidney, and lung.[82] Sequential administration of HAdv5 and BAdv3 vectors also overcomes vector immunity in an immunocompetent mouse model of breast cancer,[83] and BAdv3 and HAdv5 vector genomes have shown similar persistence in human and nonhuman cell lines.[82] Thus, BAdv3 vectors are an attractive alternative to HAdv vectors to effectively immunize individuals with high levels of preexisting HAdv immunity. Because sialic acid is the primary receptor for BAdv, this vector-based vaccine platform should be ideal for intranasal immunization.[36]

Here, we demonstrate that the BAdv nasal vaccine platform expressing the Mtb Ag85B-p25 epitope in combination with

Figure 7. BAdv^{85C5} booster induces stronger cytokine-positive T cells and effector (T_{EM}) and memory T cells (T_{CM}) in BCG-vaccinated mice following Mtb challenge

(A–D) Lungs and spleens of mice vaccinated and challenged as in Figure 6B were stained for CD4 and CD8 T cells expressing IFN-γ and IL-2 and analyzed using flow cytometry (****$p < 0.001$; ordinary 1-way ANOVA). Arrowheads indicate BAdv^{85C5}-induced T cell expansion. Flow cytometry data presented for 1 of 2 similar experiments integrated in Figure 6C.

(E–H) The lungs and spleen of mice vaccinated and challenged as in Figure 6B were stained for CD4 and CD8 T_{EM} and T_{CM} followed by flow cytometric analysis (*$p < 0.01$, ***,****$p < 0.001$, ordinary 1-way ANOVA). Arrows indicate BAdv^{85C5}-induced T cell expansion. T_{RMs} (CD4$^+$CD103$^+$CD69$^+$) on day 21 for post-vaccination (vax) and day 60 post-Mtb challenge are shown in Figure S7.

AIP-C5 generates significant protection against Mtb in mice. We have previously shown that APC processing and presentation of mycobacterial antigens is critical for vaccine-mediated anti-TB immunity.[3,5,84] While BCG and WT-Mtb evade phagolysosome fusion, BCG overexpressing Ag85B (BCG^{85B}), Ag85B plus AIP-C5 (BCG^{85BC5}), or *sapM/fbpA* gene knockouts of Mtb (Δ*fbpA-ΔsapM-Mtb*) are delivered to mouse APC lysosomes to generate peptides that activate CD4 T cells *ex vivo*.[3,8,85] Both BCG^{85B} and BCG^{85BC5} induce robust activation of Ag85-p25 epitope-specific CD4 T cells in mice after vaccination and Mtb challenge.[5,8] However, a high risk of lung inflammation precludes intranasal administration of recombinant BCG vaccines in infants.

Because DCs play a pivotal role during vaccination, we evaluated gene expression in BAdv^{85C5}-infected DCs in comparison with HAdv^{85C5}. Interestingly, BAdv^{85C5} induced significant upregulation of multiple genes involved in the sorting of vaccine-containing endosomes to lysosomes and genes regulating antigen processing (Figures 2F and 2G). These genes included the galectins *Lgals-3* and *Lgals-8,* which are associated with the vesicular transport of Adv from the endosome to the nuclear pore complex during autophagy;[45] the endosome trafficking proteins *Gabarap*, *Rab7*, *LAMP1*, *LAMP2*, *CD63*, and *CD53*; and the antigen-presentation molecules *B2m*, *H2-D1*, and *CTSs*. These findings indicate that BAdv^{85C5} enhances the ability of DCs to present the antigen to T cells, a key event during the expansion of T_H cell responses.

Based on these findings, we further investigated the mechanism(s) underlying BAdv^{85C5} vaccine-induced immunogenicity. Previous studies have shown that *Lgals-8* plays a role during WT-HAdv modulation of autophagy, reducing antigen presentation in human epithelial cells.[48] Galectins participate at various levels of autophagy; *Lgals-8* inhibits mammalian target of rapamycin (mTOR)-inducing autophagy;[39] *Lgals-3* regulates lysosome stability through lysophagy;[60,66] and WT HAdv modulates autophagy through a Nedd4.2 pathway, reducing antigen presentation.[48] BAdv^{85C5} may augment autophagy and antigen presentation through the induction of both *Lgals-3 and Lgals-8*; however, additional studies are required to determine whether *Lgals-8* synergizes to activate autophagy. Our initial studies using BAdv^{85C5} and HAdv^{85C5} revealed reduced antigen presentation to CD4 T cells when *ATG7*KO-DCs were used (Figure 4A). Inhibition of autophagy in human macrophages also reduced antigen presentation (Figure 4D). Although HAdv85-infected DC antigen presentation was demonstrable, the addition of AIP-C5 in HAdv^{85C5} significantly increased antigen presentation. Thus, co-expression of AIP-C5 with the Ag85B-p25 epitope not only bypassed the ability of HAdv to interfere with autophagy but it also enhanced the antigen presentation ability of BAdv^{85C5}-infected DCs. BAdv^{85C5} induced robust *Lgals-3* and *Lgals-8* expression compared to HAdv^{85C5} (Figures 5A and 5B). Because siRNA blockade led to the downregulation of antigen presentation, BAdv^{85C5} induction of *Lgals-3* and *Lgals-8* ostensibly facilitates antigen presentation (Figures 5C and 5D).

Consistent with our previous observation that the induction of autophagy enhances MHC class II-dependent antigen presentation by mycobacteria-infected DCs,[5] BAdv^{85C5}-infected DCs upregulated several genes, which likely facilitated autophagy-dependent antigen presentation. Different genes are induced for specific types of autophagy; *LAMP2* participates during chaperone-mediated autophagy when soluble proteins of cytosol are internalized into lysosomes,[86,87] and *Gabarap* (LC3 family) and *Rab7* are involved during selective autophagy[88] and autophagolysosome fusion, respectively. Because multiple immunoregulatory genes were expressed at lower levels following the infection of *ATG7*KO-DCs with BAdv^{85C5} compared to WT-DCs (Figure S3), the signaling pathways that deliver BAdv^{85C5} into autophagolysosomes should be investigated further. Our findings define a CTS-dependent mechanism through which BAdv^{85C5}-infected DCs demonstrate increased immunogenicity relative to HAdv^{85C5}.

BAdv^{85C5} enhanced CTS gene expression and protein synthesis compared to HAdv^{85C5} (Figures 5E and 5F). CTSs play a major role during antigenic peptide production due to the acidic pH of the lysosomes. For example, CTSD cleaves mycobacterial Ag85B to produce the p25 epitope, which is then presented to CD4 T cells.[3] CTSB, CTSS, and CTSL play a pivotal role in digesting antigens and loading microbial peptides into the groove of MHC class II.[64] Our pharmacological blockade of CTSs led to a near-abrogation of antigen presentation by BAdv^{85C5} and HAdv^{85C5} in infected DCs, validating the observed gene expression profiles (Figure 5G). Earlier studies have indicated a potential bactericidal effect of CTSs. CTSG induces the degradation of Mtb within THP-1 macrophages, and CTSB, CTSS, or CTSL blockade enhances Mtb growth in human macrophages.[89,90] Both BAdv85 and HAdv^{85C5} exerted a bactericidal effect against Mtb in mouse macrophages, suggesting that perhaps CTSs mediate this effect (Figures 4F and 4G).

These data indicate that relative to HAdv^{85C5}, BAdv^{85C5} more robustly enhances the lysosomal production of the Ag85B-p25 epitope to boost DC immunogenicity. mTOR is a major negative regulator of autophagy that controls the accumulation of DCs in the lungs and governs the programming of their metabolomes.[91] Because BAdv^{85C5} induced an upregulation of genes in DCs mainly in autophagy pathways (Figures 2, 3, 4, and 5), we propose that BAdv^{85C5} may confer superior antigen-mediated activation of T cells to lung DC populations, particularly when administered intranasally. Notably, the modified vaccinia Ankara (MVA) vaccine induces apoptosis of DCs in draining lymph nodes,[92] which is a possible reason for the failure of MVA85A to protect against TB in children. In our studies, BAdv^{85C5} was rapidly internalized into DCs (Figure 3), facilitating sustained and robust antigen presentation, with DCs remaining fully viable during *in vitro* assays (Figure 4E).

Consistent with the *in vitro* immunogenicity data, BAdv^{85C5} showed a marked protective effect in mice exposed to Mtb and induced a marked expansion of tetramer-positive CD4 T cells. When given as a single nasal vaccine, BAdv^{85C5} induced robust gene expression in the lungs and BAL cells of mice compared to HAdv^{85C5} (Figure 6A). When given as a booster following BCG, the vaccine also induced a ~1.4-log reduction of Mtb burden in the lungs compared to BCG alone (Figures 6B and 6C). For a single dose of a single epitope with a nasal booster vaccine, this appears to be the best level of protection in mice reported for any Adv vaccine for tuberculosis. Furthermore, because a single dose of a nasal vaccine alone reduced Mtb burden in both the lungs

and spleen, this vaccine strategy may also protect adults at risk for TB.

Immunity against TB is multifactorial, including T_H1-immunity facilitated by cytokine-secreting CD4 and CD8 T cells, a variety of other innate T cells, neutrophils, myeloid cells, and antibodies. Figure 7 illustrates that the BAdv^{85C5} vaccine induced an expansion of IFN-γ- and IL-2-secreting CD4 and CD8 T cells in both BCG-vaccinated mice and those receiving only the BAdv^{85C5} vaccine. Most TB vaccines induce memory T cells, which can be classified into an early T_{EM} response followed by a longer-lasting T_{CM} response. Interestingly, BCG vaccine is a poor inducer of T_{CM} response in mice,[74] although recombinant BCG vaccines induce a stronger T_{CM} response in mice correlating with superior protection against TB.[8,93] Although the role of T_{CM} response in protecting against primary exposure to Mtb is debated, it appears that T_{CM} cells play a major role in defending against reinfection and reactivation of Mtb. For example, HIV-induced CD4 T cell depletion predisposes Mtb to reactivation, implying that at least CD4 T_{CM} cells persist in a resting stage in those vaccinated with BCG or exposed to Mtb. These resting T_{CM} cells can rapidly expand into T_{EM} cells to contain Mtb after exposure. In our investigation, BAdv^{85C5} vaccination led to an expansion of both T_{EM} and T_{CM} cells in BCG-vaccinated mice (Figure 7). Curiously, BAdv^{85C5} given alone expanded T_{CM} cells in the spleen (Figure 7), indicating that the BAdv^{85C5} vaccine can be used even among adults to activate T_{CM} cells. This is significant because, at least in the mouse model, BCG seems to be a poor inducer of T_{CM} response.[74] Intradermal BCG vaccination of neonates followed by a nasal booster with BAdv^{85C5} may stimulate longer-lasting immunity, while adults exposed to index cases of TB may be protected by the BAdv^{85C5} vaccine alone.

BCG revaccination of healthy volunteers reduces skin test conversion, but whether it affects TB susceptibility remains unclear. Intranasal BCG is not feasible, but we propose that a BAdv^{85C5} nasal vaccine can strengthen the lung compartment to resist aerosol infection with Mtb. Supporting this concept, the BAdv^{85C5} booster enhanced T_{RM} responses in the lungs of BCG-vaccinated mice before and after Mtb exposure (Figure S7). This is a clinically significant finding, as human and mouse neonates both show a reduced expansion of T_{RM} cells after influenza infection.[21] Others have suggested that during RSV vaccination, TLR activation may help in overcoming the hypo-responsiveness of T_{RM} cells in the lungs.[94] In this context, we recall that AIP-C5 activates TLR-2 in both mouse and human APCs, inducing autophagy.[8] Although additional studies are required, we consider that the TLR2-dependent adjuvant effect of AIP-C5 may contribute to the robust T cell responses in the lungs following BAdv^{85C5} vaccination, which will likely augment neonatal lung immunity when given as a nasal vaccine.

In summary, the BAdv vaccine platform enables the expression of an Mtb immunogenic peptide and activates *Lgals-3 and Lgals-8*-dependent autophagy. This platform led to robust antigen presentation by both mouse DCs and human macrophages, resulting in excellent protection against TB. Autophagy-mediated antigen presentation through a BAdv vaccine platform expressing multivalent immunogenic proteins of Mtb may facilitate future designs of more potent mucosal TB vaccines for children and adults.

Limitations of the study

We have demonstrated the efficacy of BAdv^{85C5} vaccine using 4- to 6-week-old C57BL/6 mice that have an immune system resembling that of human infants. However, a neonatal mouse model would be ideal for an additional evaluation of the vaccine, given that BCG is provided after birth. We also need to test nasal booster vaccine months after BCG vaccine using neonatal mice and evaluate gene expression studies post-TB challenges. The potential of the full 85B antigen with or without other immunogenic antigens of Mtb in the BAdv vaccine platform should be explored.

STAR★METHODS

Detailed methods are provided in the online version of this paper and include the following:

- KEY RESOURCES TABLE
- RESOURCE AVAILABILITY
  - Lead contact
  - Materials availability
  - Data and code availability
- EXPERIMENTAL MODEL AND SUBJECT DETAILS
  - Mice
  - Ethics statement
  - Cell lines
  - Primary cells
- METHOD DETAILS
  - Isolation and cultivation of primary mouse marophages and DCs (APCs)
  - Bacterial strains and culture conditions
  - Adenoviral vectors and culture conditions
  - Isolation and cultivation of primary human macrophages from peripheral blood samples
  - Infection of APCs with Adv vectors and vaccines
  - RNaseq analysis
  - qPCR assay for gene expression in mouse bone marrow derived dendritic cells
  - *Ex vivo* Mtb Ag85B antigen presentation to CD4 T cells
  - siRNA knockdown of BAdv/HAdv vectors-infected APCs
  - Evaluation of virus containing endosomes and their co-localization with autophagolysosomes using antibodies and Cy3 labeled BAdv vector and vaccine in DCs
  - Mouse vaccine experiments
  - Post Mtb challenge flow cytometry for TRMs
  - Flow cytometry analysis
  - Post vaccination and post Mtb challenge flow cytometry for TRMs
  - Western blots: 'Wes Protein Simple' western assay / Wes analysis of proteins in lysates of DCs
- QUANTIFICATION AND STATISTICAL ANALYSIS

SUPPLEMENTAL INFORMATION

Supplemental information can be found online at https://doi.org/10.1016/j.xcrm.2021.100372.

ACKNOWLEDGMENTS

This work was supported in part by NIH grant AI122070 (principal investigator, C.J.) and supporting funds from the Houston Methodist Academy of Medicine. This work was partially supported by the Hatch funds (principal investigator, S.K.M.). We thank Ahmed Hassan for generating some of the Adv vectors. We are grateful to Drs. Pejerrey and McConnell for editing the manuscript.

AUTHOR CONTRIBUTIONS

A.K., E.E.S., V.K.S., and A.M. performed the experiments; S.D.-E., S.N., and K.J.S. analyzed the flow cytometry data; D.H.C., M.C., and J.W. provided the research materials; C.J. and S.K.M. designed the experiments and wrote the manuscript.

DECLARATION OF INTERESTS

The authors declare no competing interests.

Received: June 22, 2020
Revised: February 16, 2021
Accepted: July 19, 2021
Published: August 17, 2021

REFERENCES

1. Mangtani, P., Abubakar, I., Ariti, C., Beynon, R., Pimpin, L., Fine, P.E., Rodrigues, L.C., Smith, P.G., Lipman, M., Whiting, P.F., et al. (2014). Protection by BCG vaccine against tuberculosis: a systematic review of randomized controlled trials. Clin. Infect. Dis. *58*, 470–480.
2. Pancholi, P., Mirza, A., Bhardwaj, N., and Steinman, R.M. (1993). Sequestration from immune CD4+ T cells of mycobacteria growing in human macrophages. Science *260*, 984–986.
3. Singh, C.R., Moulton, R.A., Armitige, L.Y., Bidani, A., Snuggs, M., Dhandayuthapani, S., Hunter, R.L., and Jagannath, C. (2006). Processing and presentation of a mycobacterial antigen 85B epitope by murine macrophages is dependent on the phagosomal acquisition of vacuolar proton ATPase and in situ activation of cathepsin D. J. Immunol. *177*, 3250–3259.
4. Singh, C.R., Bakhru, P., Khan, A., Li, Q.B., and Jagannath, C. (2011). Cutting edge: nicastrin and related components of γ-secretase generate a peptide epitope facilitating immune recognition of intracellular mycobacteria, through MHC class II-dependent priming of T cells. J. Immunol. *187*, 5495–5499.
5. Jagannath, C., Lindsey, D.R., Dhandayuthapani, S., Xu, Y., Hunter, R.L., Jr., and Eissa, N.T. (2009). Autophagy enhances the efficacy of BCG vaccine by increasing peptide presentation in mouse dendritic cells. Nat. Med. *15*, 267–276.
6. Bakhru, P. (2012). Induction of stronger and long lasting vaccine mediated immunity to tuberculosis (University of Texas Health Sciences Center), PhD thesis.
7. Bakhru, P., Sirisaengtaksin, N., Soudani, E., Mukherjee, S., Khan, A., and Jagannath, C. (2013). BCG vaccine mediated reduction in MHC-II expression of macrophages and dendritic cells can be reversed using activation of Toll-like receptors 7 and 9. Cell. Immunol. *287*, 53–61.
8. Khan, A., Bakhru, P., Saikolappan, S., Das, K., Soudani, E., Singh, C.R., Estrella, J.L., Zhang, D., Pasare, C., Ma, Y., et al. (2019). An autophagy-inducing and TLR-2 activating BCG vaccine induces a robust protection against tuberculosis in mice. NPJ Vaccines *4*, 34.
9. Gengenbacher, M., Nieuwenhuizen, N., Vogelzang, A., Liu, H., Kaiser, P., Schuerer, S., Lazar, D., Wagner, I., Mollenkopf, H.J., and Kaufmann, S.H. (2016). Deletion of nuoG from the Vaccine Candidate Mycobacterium bovis BCG ΔureC:hly Improves Protection against Tuberculosis. mBio *7*, e00679-16.
10. Ramzan, M., Ali, S.M., Malik, A., Zaka-ur-Rab, Z., and Shahab, T. (2009). Frequency of HIV infection amongst children with disseminated tuberculosis and tuberculous meningitis in Aligarh (North India) - a low HIV prevalence area. J. Coll. Physicians Surg. Pak. *19*, 566–569.
11. Santosuosso, M., McCormick, S., Zhang, X., Zganiacz, A., and Xing, Z. (2006). Intranasal boosting with an adenovirus-vectored vaccine markedly enhances protection by parenteral Mycobacterium bovis BCG immunization against pulmonary tuberculosis. Infect. Immun. *74*, 4634–4643.
12. Xing, Z., McFarland, C.T., Sallenave, J.M., Izzo, A., Wang, J., and McMurray, D.N. (2009). Intranasal mucosal boosting with an adenovirus-vectored vaccine markedly enhances the protection of BCG-primed guinea pigs against pulmonary tuberculosis. PLoS ONE *4*, e5856.
13. Hoft, D.F., Blazevic, A., Stanley, J., Landry, B., Sizemore, D., Kpamegan, E., Gearhart, J., Scott, A., Kik, S., Pau, M.G., et al. (2012). A recombinant adenovirus expressing immunodominant TB antigens can significantly enhance BCG-induced human immunity. Vaccine *30*, 2098–2108.
14. van Zyl-Smit, R.N., Esmail, A., Bateman, M.E., Dawson, R., Goldin, J., van Rikxoort, E., Douoguih, M., Pau, M.G., Sadoff, J.C., McClain, J.B., et al. (2017). Safety and Immunogenicity of Adenovirus 35 Tuberculosis Vaccine Candidate in Adults with Active or Previous Tuberculosis. A Randomized Trial. Am. J. Respir. Crit. Care Med. *195*, 1171–1180.
15. Ahi, Y.S., Bangari, D.S., and Mittal, S.K. (2011). Adenoviral vector immunity: its implications and circumvention strategies. Curr. Gene Ther. *11*, 307–320.
16. Fausther-Bovendo, H., and Kobinger, G.P. (2014). Pre-existing immunity against Ad vectors: humoral, cellular, and innate response, what's important? Hum. Vaccin. Immunother. *10*, 2875–2884.
17. Florido, M., Pillay, R., Gillis, C.M., Xia, Y., Turner, S.J., Triccas, J.A., Stambas, J., and Britton, W.J. (2015). Epitope-specific CD4+, but not CD8+, T-cell responses induced by recombinant influenza A viruses protect against Mycobacterium tuberculosis infection. Eur. J. Immunol. *45*, 780–793.
18. Florido, M., Muflihah, H., Lin, L.C.W., Xia, Y., Sierro, F., Palendira, M., Feng, C.G., Bertolino, P., Stambas, J., Triccas, J.A., et al. (2018). Pulmonary immunization with a recombinant influenza A virus vaccine induces lung-resident CD4(+) memory T cells that are associated with protection against tuberculosis. Mucosal Immunol. *11*, 1743–1752.
19. Darrah, P.A., DiFazio, R.M., Maiello, P., Gideon, H.P., Myers, A.J., Rodgers, M.A., Hackney, J.A., Lindenstrom, T., Evans, T., Scanga, C.A., et al. (2019). Boosting BCG with proteins or rAd5 does not enhance protection against tuberculosis in rhesus macaques. NPJ Vaccines *4*, 21.
20. Tameris, M.D., Hatherill, M., Landry, B.S., Scriba, T.J., Snowden, M.A., Lockhart, S., Shea, J.E., McClain, J.B., Hussey, G.D., Hanekom, W.A., et al.; MVA85A 020 Trial Study Team (2013). Safety and efficacy of MVA85A, a new tuberculosis vaccine, in infants previously vaccinated with BCG: a randomised, placebo-controlled phase 2b trial. Lancet *381*, 1021–1028.
21. Zens, K.D., Chen, J.K., Guyer, R.S., Wu, F.L., Cvetkovski, F., Miron, M., and Farber, D.L. (2017). Reduced generation of lung tissue-resident memory T cells during infancy. J. Exp. Med. *214*, 2915–2932.
22. Saso, A., and Kampmann, B. (2017). Vaccine responses in newborns. Semin. Immunopathol. *39*, 627–642.
23. Yu, J.C., Khodadadi, H., Malik, A., Davidson, B., Salles, É.D.S.L., Bhatia, J., Hale, V.L., and Baban, B. (2018). Innate Immunity of Neonates and Infants. Front. Immunol. *9*, 1759.
24. Singh, N., Pandey, A., Jayashankar, L., and Mittal, S.K. (2008). Bovine adenoviral vector-based H5N1 influenza vaccine overcomes exceptionally high levels of pre-existing immunity against human adenovirus. Mol. Ther. *16*, 965–971.
25. Sharma, A., Bangari, D.S., Tandon, M., Hogenesch, H., and Mittal, S.K. (2010). Evaluation of innate immunity and vector toxicity following

inoculation of bovine, porcine or human adenoviral vectors in a mouse model. Virus Res. *153*, 134–142.

26. Bangari, D.S., and Mittal, S.K. (2006). Current strategies and future directions for eluding adenoviral vector immunity. Curr. Gene Ther. *6*, 215–226.
27. Vemula, S.V., and Mittal, S.K. (2010). Production of adenovirus vectors and their use as a delivery system for influenza vaccines. Expert Opin. Biol. Ther. *10*, 1469–1487.
28. Zhu, J., Huang, X., and Yang, Y. (2007). Innate immune response to adenoviral vectors is mediated by both Toll-like receptor-dependent and -independent pathways. J. Virol. *81*, 3170–3180.
29. Cao, W., Liepkalns, J.S., Hassan, A.O., Kamal, R.P., Hofstetter, A.R., Amoah, S., Kim, J.H., Reber, A.J., Stevens, J., Katz, J.M., et al. (2016). A highly immunogenic vaccine against A/H7N9 influenza virus. Vaccine *34*, 744–749.
30. Hoelscher, M.A., Garg, S., Bangari, D.S., Belser, J.A., Lu, X., Stephenson, I., Bright, R.A., Katz, J.M., Mittal, S.K., and Sambhara, S. (2006). Development of adenoviral-vector-based pandemic influenza vaccine against antigenically distinct human H5N1 strains in mice. Lancet *367*, 475–481.
31. Hoelscher, M.A., Jayashankar, L., Garg, S., Veguilla, V., Lu, X., Singh, N., Katz, J.M., Mittal, S.K., and Sambhara, S. (2007). New pre-pandemic influenza vaccines: an egg- and adjuvant-independent human adenoviral vector strategy induces long-lasting protective immune responses in mice. Clin. Pharmacol. Ther. *82*, 665–671.
32. Smaill, F., Jeyanathan, M., Smieja, M., Medina, M.F., Thanthrige-Don, N., Zganiacz, A., Yin, C., Heriazon, A., Damjanovic, D., Puri, L., et al. (2013). A human type 5 adenovirus-based tuberculosis vaccine induces robust T cell responses in humans despite preexisting anti-adenovirus immunity. Sci. Transl. Med. *5*, 205ra134.
33. Barouch, D.H., Tomaka, F.L., Wegmann, F., Stieh, D.J., Alter, G., Robb, M.L., Michael, N.L., Peter, L., Nkolola, J.P., Borducchi, E.N., et al. (2018). Evaluation of a mosaic HIV-1 vaccine in a multicentre, randomised, double-blind, placebo-controlled, phase 1/2a clinical trial (APPROACH) and in rhesus monkeys (NHP 13-19). Lancet *392*, 232–243.
34. Van Kampen, K.R., Shi, Z., Gao, P., Zhang, J., Foster, K.W., Chen, D.T., Marks, D., Elmets, C.A., and Tang, D.C. (2005). Safety and immunogenicity of adenovirus-vectored nasal and epicutaneous influenza vaccines in humans. Vaccine *23*, 1029–1036.
35. Ledgerwood, J.E., DeZure, A.D., Stanley, D.A., Coates, E.E., Novik, L., Enama, M.E., Berkowitz, N.M., Hu, Z., Joshi, G., Ploquin, A., et al. (2017). Chimpanzee Adenovirus Vector Ebola Vaccine. N. Engl. J. Med. *376*, 928–938.
36. Sayedahmed, E.E., Hassan, A.O., Kumari, R., Cao, W., Gangappa, S., York, I., Sambhara, S., and Mittal, S.K. (2018). A bovine adenoviral vector-based H5N1 influenza -vaccine provides enhanced immunogenicity and protection at a significantly low dose. Mol. Ther. Methods Clin. Dev. *10*, 210–222.
37. Chen, M., Hong, M.J., Sun, H., Wang, L., Shi, X., Gilbert, B.E., Corry, D.B., Kheradmand, F., and Wang, J. (2014). Essential role for autophagy in the maintenance of immunological memory against influenza infection. Nat. Med. *20*, 503–510.
38. Pérez-Montesinos, G., López-Ortega, O., Piedra-Reyes, J., Bonifaz, L.C., and Moreno, J. (2017). Dynamic Changes in the Intracellular Association of Selected Rab Small GTPases with MHC Class II and DM during Dendritic Cell Maturation. Front. Immunol. *8*, 340.
39. Jia, J., Abudu, Y.P., Claude-Taupin, A., Gu, Y., Kumar, S., Choi, S.W., Peters, R., Mudd, M.H., Allers, L., Salemi, M., et al. (2018). Galectins Control mTOR in Response to Endomembrane Damage. Mol. Cell *70*, 120–135.e8.
40. Li, F.Y., Wang, S.F., Bernardes, E.S., and Liu, F.T. (2020). Galectins in Host Defense Against Microbial Infections. Adv. Exp. Med. Biol. *1204*, 141–167.
41. Münz, C. (2015). Of LAP, CUPS, and DRibbles - Unconventional Use of Autophagy Proteins for MHC Restricted Antigen Presentation. Front. Immunol. *6*, 200.
42. Schaaf, M.B., Keulers, T.G., Vooijs, M.A., and Rouschop, K.M. (2016). LC3/GABARAP family proteins: autophagy-(un)related functions. FASEB J. *30*, 3961–3978.
43. Segura, E., and Amigorena, S. (2015). Cross-Presentation in Mouse and Human Dendritic Cells. Adv. Immunol. *127*, 1–31.
44. Leopold, P.L., Ferris, B., Grinberg, I., Worgall, S., Hackett, N.R., and Crystal, R.G. (1998). Fluorescent virions: dynamic tracking of the pathway of adenoviral gene transfer vectors in living cells. Hum. Gene Ther. *9*, 367–378.
45. Hendrickx, R., Stichling, N., Koelen, J., Kuryk, L., Lipiec, A., and Greber, U.F. (2014). Innate immunity to adenovirus. Hum. Gene Ther. *25*, 265–284.
46. Bailey, C.J., Crystal, R.G., and Leopold, P.L. (2003). Association of adenovirus with the microtubule organizing center. J. Virol. *77*, 13275–13287.
47. Maier, O., Marvin, S.A., Wodrich, H., Campbell, E.M., and Wiethoff, C.M. (2012). Spatiotemporal dynamics of adenovirus membrane rupture and endosomal escape. J. Virol. *86*, 10821–10828.
48. Montespan, C., Marvin, S.A., Austin, S., Burrage, A.M., Roger, B., Rayne, F., Faure, M., Campell, E.M., Schneider, C., Reimer, R., et al. (2017). Multi-layered control of Galectin-8 mediated autophagy during adenovirus cell entry through a conserved PPxY motif in the viral capsid. PLoS Pathog. *13*, e1006217.
49. Sharma, P.K., Dmitriev, I.P., Kashentseva, E.A., Raes, G., Li, L., Kim, S.W., Lu, Z.H., Arbeit, J.M., Fleming, T.P., Kaliberov, S.A., et al. (2018). Development of an adenovirus vector vaccine platform for targeting dendritic cells. Cancer Gene Ther. *25*, 27–38.
50. Rodo, M.J., Rozot, V., Nemes, E., Dintwe, O., Hatherill, M., Little, F., and Scriba, T.J. (2019). A comparison of antigen-specific T cell responses induced by six novel tuberculosis vaccine candidates. PLoS Pathog. *15*, e1007643.
51. Lee, H.K., Mattei, L.M., Steinberg, B.E., Alberts, P., Lee, Y.H., Chervonsky, A., Mizushima, N., Grinstein, S., and Iwasaki, A. (2010). In vivo requirement for Atg5 in antigen presentation by dendritic cells. Immunity *32*, 227–239.
52. Ramachandra, L., Noss, E., Boom, W.H., and Harding, C.V. (1999). Phagocytic processing of antigens for presentation by class II major histocompatibility complex molecules. Cell. Microbiol. *1*, 205–214.
53. Ramachandra, L., Noss, E., Boom, W.H., and Harding, C.V. (2001). Processing of Mycobacterium tuberculosis antigen 85B involves intraphagosomal formation of peptide-major histocompatibility complex II complexes and is inhibited by live bacilli that decrease phagosome maturation. J. Exp. Med. *194*, 1421–1432.
54. Soualhine, H., Deghmane, A.E., Sun, J., Mak, K., Talal, A., Av-Gay, Y., and Hmama, Z. (2007). Mycobacterium bovis bacillus Calmette-Guérin secreting active cathepsin S stimulates expression of mature MHC class II molecules and antigen presentation in human macrophages. J. Immunol. *179*, 5137–5145.
55. Saini, N.K., Baena, A., Ng, T.W., Venkataswamy, M.M., Kennedy, S.C., Kunnath-Velayudhan, S., Carreño, L.J., Xu, J., Chan, J., Larsen, M.H., et al. (2016). Suppression of autophagy and antigen presentation by Mycobacterium tuberculosis PE_PGRS47. Nat. Microbiol. *1*, 16133.
56. Nishida, Y., Arakawa, S., Fujitani, K., Yamaguchi, H., Mizuta, T., Kanaseki, T., Komatsu, M., Otsu, K., Tsujimoto, Y., and Shimizu, S. (2009). Discovery of Atg5/Atg7-independent alternative macroautophagy. Nature *461*, 654–658.
57. Trinh, H.V., Grossmann, J., Gehrig, P., Roschitzki, B., Schlapbach, R., Greber, U.F., and Hemmi, S. (2013). iTRAQ-Based and Label-Free Proteomics Approaches for Studies of Human Adenovirus Infections. Int. J. Proteomics *2013*, 581862.

58. Baba, T., Toth, D.J., Sengupta, N., Kim, Y.J., and Balla, T. (2019). Phosphatidylinositol 4,5-bisphosphate controls Rab7 and PLEKHM1 membrane cycling during autophagosome-lysosome fusion. EMBO J. *38*, e100312.

59. Thurston, T.L., Wandel, M.P., von Muhlinen, N., Foeglein, A., and Randow, F. (2012). Galectin 8 targets damaged vesicles for autophagy to defend cells against bacterial invasion. Nature *482*, 414–418.

60. Jia, J., Claude-Taupin, A., Gu, Y., Choi, S.W., Peters, R., Bissa, B., Mudd, M.H., Allers, L., Pallikkuth, S., Lidke, K.A., et al. (2020). Galectin-3 Coordinates a Cellular System for Lysosomal Repair and Removal. Dev. Cell *52*, 69–87.e8.

61. Chauhan, S., Kumar, S., Jain, A., Ponpuak, M., Mudd, M.H., Kimura, T., Choi, S.W., Peters, R., Mandell, M., Bruun, J.A., et al. (2016). TRIMs and Galectins Globally Cooperate and TRIM16 and Galectin-3 Co-direct Autophagy in Endomembrane Damage Homeostasis. Dev. Cell *39*, 13–27.

62. Weng, I.C., Chen, H.L., Lo, T.H., Lin, W.H., Chen, H.Y., Hsu, D.K., and Liu, F.T. (2018). Cytosolic galectin-3 and -8 regulate antibacterial autophagy through differential recognition of host glycans on damaged phagosomes. Glycobiology *28*, 392–405.

63. Lee, J.A., Sinkovits, R.S., Mock, D., Rab, E.L., Cai, J., Yang, P., Saunders, B., Hsueh, R.C., Choi, S., Subramaniam, S., and Scheuermann, R.H.; Alliance for Cellular Signaling (2006). Components of the antigen processing and presentation pathway revealed by gene expression microarray analysis following B cell antigen receptor (BCR) stimulation. BMC Bioinformatics *7*, 237.

64. Katunuma, N., Matsunaga, Y., Himeno, K., and Hayashi, Y. (2003). Insights into the roles of cathepsins in antigen processing and presentation revealed by specific inhibitors. Biol. Chem. *384*, 883–890.

65. Huggins, M.A., Sjaastad, F.V., Pierson, M., Kucaba, T.A., Swanson, W., Staley, C., Weingarden, A.R., Jensen, I.J., Danahy, D.B., Badovinac, V.P., et al. (2019). Microbial Exposure Enhances Immunity to Pathogens Recognized by TLR2 but Increases Susceptibility to Cytokine Storm through TLR4 Sensitization. Cell Rep. *28*, 1729–1743.e5.

66. Yao, R.-Q., Ren, C., Xia, Z.-F., and Yao, Y.-M. (2021). Organelle-specific autophagy in inflammatory diseases: a potential therapeutic target underlying the quality control of multiple organelles. Autophagy *17*, 385–401.

67. Tamura, T., Ariga, H., Kinashi, T., Uehara, S., Kikuchi, T., Nakada, M., Tokunaga, T., Xu, W., Kariyone, A., Saito, T., et al. (2004). The role of antigenic peptide in CD4+ T helper phenotype development in a T cell receptor transgenic model. Int. Immunol. *16*, 1691–1699.

68. Kaveh, D.A., Bachy, V.S., Hewinson, R.G., and Hogarth, P.J. (2011). Systemic BCG immunization induces persistent lung mucosal multifunctional CD4 T(EM) cells which expand following virulent mycobacterial challenge. PLoS ONE *6*, e21566.

69. Wherry, E.J., Teichgräber, V., Becker, T.C., Masopust, D., Kaech, S.M., Antia, R., von Andrian, U.H., and Ahmed, R. (2003). Lineage relationship and protective immunity of memory CD8 T cell subsets. Nat. Immunol. *4*, 225–234.

70. Jabbari, A., and Harty, J.T. (2006). Secondary memory CD8+ T cells are more protective but slower to acquire a central-memory phenotype. J. Exp. Med. *203*, 919–932.

71. Gray, J.I., Westerhof, L.M., and MacLeod, M.K.L. (2018). The roles of resident, central and effector memory CD4 T-cells in protective immunity following infection or vaccination. Immunology *154*, 574–581.

72. Peters, W., Scott, H.M., Chambers, H.F., Flynn, J.L., Charo, I.F., and Ernst, J.D. (2001). Chemokine receptor 2 serves an early and essential role in resistance to Mycobacterium tuberculosis. Proc. Natl. Acad. Sci. USA *98*, 7958–7963.

73. Hoft, S.G., Sallin, M.A., Kauffman, K.D., Sakai, S., Ganusov, V.V., and Barber, D.L. (2019). The Rate of CD4 T Cell Entry into the Lungs during Mycobacterium tuberculosis Infection Is Determined by Partial and Opposing Effects of Multiple Chemokine Receptors. Infect. Immun. *87*, e00841-18.

74. Orme, I.M. (2010). The Achilles heel of BCG. Tuberculosis (Edinb.) *90*, 329–332.

75. Kumar, B.V., Ma, W., Miron, M., Granot, T., Guyer, R.S., Carpenter, D.J., Senda, T., Sun, X., Ho, S.H., Lerner, H., et al. (2017). Human Tissue-Resident Memory T Cells Are Defined by Core Transcriptional and Functional Signatures in Lymphoid and Mucosal Sites. Cell Rep. *20*, 2921–2934.

76. Ogongo, P., Porterfield, J.Z., and Leslie, A. (2019). Lung Tissue Resident Memory T-Cells in the Immune Response to *Mycobacterium tuberculosis*. Front. Immunol. *10*, 992.

77. Thompson, E.A., Darrah, P.A., Foulds, K.E., Hoffer, E., Caffrey-Carr, A., Norenstedt, S., Perbeck, L., Seder, R.A., Kedl, R.M., and Loré, K. (2019). Monocytes Acquire the Ability to Prime Tissue-Resident T Cells via IL-10-Mediated TGF-β Release. Cell Rep. *28*, 1127–1135.e4.

78. Bangari, D.S., Sharma, A., and Mittal, S.K. (2005). Bovine adenovirus type 3 internalization is independent of primary receptors of human adenovirus type 5 and porcine adenovirus type 3. Biochem. Biophys. Res. Commun. *331*, 1478–1484.

79. Li, X., Bangari, D.S., Sharma, A., and Mittal, S.K. (2009). Bovine adenovirus serotype 3 utilizes sialic acid as a cellular receptor for virus entry. Virology *392*, 162–168.

80. Bangari, D.S., Shukla, S., and Mittal, S.K. (2005). Comparative transduction efficiencies of human and nonhuman adenoviral vectors in human, murine, bovine, and porcine cells in culture. Biochem. Biophys. Res. Commun. *327*, 960–966.

81. Sharma, A., Tandon, M., Ahi, Y.S., Bangari, D.S., Vemulapalli, R., and Mittal, S.K. (2010). Evaluation of cross-reactive cell-mediated immune responses among human, bovine and porcine adenoviruses. Gene Ther. *17*, 634–642.

82. Sharma, A., Bangari, D.S., Tandon, M., Pandey, A., HogenEsch, H., and Mittal, S.K. (2009). Comparative analysis of vector biodistribution, persistence and gene expression following intravenous delivery of bovine, porcine and human adenoviral vectors in a mouse model. Virology *386*, 44–54.

83. Tandon, M., Sharma, A., Vemula, S.V., Bangari, D.S., and Mittal, S.K. (2012). Sequential administration of bovine and human adenovirus vectors to overcome vector immunity in an immunocompetent mouse model of breast cancer. Virus Res. *163*, 202–211.

84. Jagannath, C., and Bakhru, P. (2012). Rapamycin-induced enhancement of vaccine efficacy in mice. Methods Mol. Biol. *821*, 295–303.

85. Saikolappan, S., Estrella, J., Sasindran, S.J., Khan, A., Armitige, L.Y., Jagannath, C., and Dhandayuthapani, S. (2012). The fbpA/sapM double knock out strain of Mycobacterium tuberculosis is highly attenuated and immunogenic in macrophages. PLoS ONE *7*, e36198.

86. Wang, B., Chen, Z., Yu, F., Chen, Q., Tian, Y., Ma, S., Wang, T., and Liu, X. (2016). Hsp90 regulates autophagy and plays a role in cancer therapy. Tumour Biol *37*, 1–6.

87. Tekirdag, K., and Cuervo, A.M. (2018). Chaperone-mediated autophagy and endosomal microautophagy: joint by a chaperone. J. Biol. Chem. *293*, 5414–5424.

88. Khaminets, A., Heinrich, T., Mari, M., Grumati, P., Huebner, A.K., Akutsu, M., Liebmann, L., Stolz, A., Nietzsche, S., Koch, N., et al. (2015). Regulation of endoplasmic reticulum turnover by selective autophagy. Nature *522*, 354–358.

89. Rivera-Marrero, C.A., Stewart, J., Shafer, W.M., and Roman, J. (2004). The down-regulation of cathepsin G in THP-1 monocytes after infection with Mycobacterium tuberculosis is associated with increased intracellular survival of bacilli. Infect. Immun. *72*, 5712–5721.

90. Pires, D., Marques, J., Pombo, J.P., Carmo, N., Bettencourt, P., Neyrolles, O., Lugo-Villarino, G., and Anes, E. (2016). Role of Cathepsins in Mycobacterium tuberculosis Survival in Human Macrophages. Sci. Rep. *6*, 32247.

91. Sinclair, C., Bommakanti, G., Gardinassi, L., Loebbermann, J., Johnson, M.J., Hakimpour, P., Hagan, T., Benitez, L., Todor, A., Machiah, D., et al. (2017). mTOR regulates metabolic adaptation of APCs in the lung and controls the outcome of allergic inflammation. Science *357*, 1014–1021.

92. Guzman, E., Cubillos-Zapata, C., Cottingham, M.G., Gilbert, S.C., Prentice, H., Charleston, B., and Hope, J.C. (2012). Modified vaccinia virus Ankara-based vaccine vectors induce apoptosis in dendritic cells draining from the skin via both the extrinsic and intrinsic caspase pathways, preventing efficient antigen presentation. J. Virol. *86*, 5452–5466.

93. Vogelzang, A., Perdomo, C., Zedler, U., Kuhlmann, S., Hurwitz, R., Gengenbacher, M., and Kaufmann, S.H. (2014). Central memory CD4+ T cells are responsible for the recombinant Bacillus Calmette-Guérin ΔureC:hly vaccine's superior protection against tuberculosis. J. Infect. Dis. *210*, 1928–1937.

94. Zhang, L., Li, H., Hai, Y., Yin, W., Li, W., Zheng, B., Du, X., Li, N., Zhang, Z., Deng, Y., et al. (2017). CpG in Combination with an Inhibitor of Notch Signaling Suppresses Formalin-Inactivated Respiratory Syncytial Virus-Enhanced Airway Hyperresponsiveness and Inflammation by Inhibiting Th17 Memory Responses and Promoting Tissue-Resident Memory Cells in Lungs. J. Virol. *91*, e02111-16.

95. van Olphen, A.L., and Mittal, S.K. (2002). Development and characterization of bovine x human hybrid cell lines that efficiently support the replication of both wild-type bovine and human adenoviruses and those with E1 deleted. J. Virol. *76*, 5882–5892.

96. Graham, F.L., Smiley, J., Russell, W.C., and Nairn, R. (1977). Characteristics of a human cell line transformed by DNA from human adenovirus type 5. J. Gen. Virol. *36*, 59–74.

97. Ng, P., Parks, R.J., Cummings, D.T., Evelegh, C.M., Sankar, U., and Graham, F.L. (1999). A high-efficiency Cre/loxP-based system for construction of adenoviral vectors. Hum. Gene Ther. *10*, 2667–2672.

98. Noblitt, L.W., Bangari, D.S., Shukla, S., Knapp, D.W., Mohammed, S., Kinch, M.S., and Mittal, S.K. (2004). Decreased tumorigenic potential of EphA2-overexpressing breast cancer cells following treatment with adenoviral vectors that express EphrinA1. Cancer Gene Ther. *11*, 757–766.

99. van Olphen, A.L., and Mittal, S.K. (1999). Generation of infectious genome of bovine adenovirus type 3 by homologous recombination in bacteria. J. Virol. Methods *77*, 125–129.

100. Sayedahmed, E.E., Kumari, R., and Mittal, S.K. (2019). Current Use of Adenovirus Vectors and Their Production Methods. Methods Mol. Biol. *1937*, 155–175.

101. Vemula, S.V., Ahi, Y.S., Swaim, A.M., Katz, J.M., Donis, R., Sambhara, S., and Mittal, S.K. (2013). Broadly protective adenovirus-based multivalent vaccines against highly pathogenic avian influenza viruses for pandemic preparedness. PLoS ONE *8*, e62496.

STAR★METHODS

KEY RESOURCES TABLE

REAGENT or RESOURCE	SOURCE	IDENTIFIER
Antibodies		
CD3	BD Biosciences	564380
CD62L	BD Biosciences	553150
CD8	BD Biosciences	551162
CD44	BD Biosciences	562464
CD4	BD Biosciences	561025
CCR7	eBioscience	12-1971-80
IFN-γ	BD Biosciences	564336
IL-2	BD Biosciences	560547
CD103	BD Biosciences	562772
CD69	BD Biosciences	740220
CD11a	BD Biosciences	740849
Rab7	Cell Signaling	9367T
LC3B	Cell Signaling	2775s
GAPDH	Cell Signaling	5174s
Gbp1	Novus Biologicals	NBP-1-31560
Bacterial and virus strains		
Mycobacterium tuberculosis Erdman	ATCC	ATCC 25177
Bovine adenovirus	ATCC	ATCC VR-639
Human Adenovirus	ATCC	ATCC VR-5
Mycobacterium bovis BCG Pasteur	ATCC	ATCC 35732
Biological samples		
Peripheral blood from Human subjects	Gulf coast regional Blood Center, Houston	NA
Chemicals, peptides, and recombinant proteins		
IMDM Media	GE Healthcare HyClone	SH30228.01
FBS	GE Healthcare HyClone	SH30070.01
Penicillin and gentamycin	GIBCO	15140148
HEPES	GIBCO	15630080
2-Mercapto ethanol	GIBCO	21985023
h-GM-CSF	BioLegend	572904
m-GM-CSF	BioLegend	576306
Histopaque 1077	Sigma	1077500ML
ACK buffer	Lonza	10548E
RPMI 1640 Medium	Sigma	R8758
RIPA buffer	Sigma	R0278
SDS	Sigma	L3771
Collagenase	Thermo Fisher Scientific	17101015
Human AB serum	Fisher	BP2525100
Kanamycin	Fisher	BP906-5
Lysotracker red	Invitrogen	L7528
Lysotracker green	Invitrogen	L7526
PMA	Sigma	P1585
Ionomycin	Sigma	I0634

(*Continued on next page*)

Continued

REAGENT or RESOURCE	SOURCE	IDENTIFIER
3-Methyl adenine	Sigma	M9281
NLLM	Tocris Bioscience	0384/10
Calpeptin	Tocris Bioscience	0448/10
E64	Tocris Bioscience	5208/10
Critical commercial assays		
Aqua (LIVE/DEAD Fixable Aqua Dead Cell Stain Kit)	Thermo Fisher Scientific	L34957
Mouse IL-2 Elisa Kit‘	BioLegend	431001
Deposited data		
RNaseq raw data	This paper	https://www.ncbi.nlm.nih.gov/sra/PRJNA745957
Experimental models: cell lines		
BB7 CD4 T cell hybridoma specific for H2-d Ag85B epitope	Gift from Dr. Cliff Hording	NA
F9A6 T cell hybridoma specific for HLA-DR1 Ag85B epitope	Gift from Dr. David Canaday	NA
Experimental models: organisms/strains		
C57BL/6 mice	Charles River	C57BL/6NCrl
Oligonucleotides		
LGALS3 siRNA	OriGene	SR302676
LGASL8 siRNA	OriGene	SR410253
Software and algorithms		
GraphPad Prism 8.0	GraphPad Software, CA, USA	NA
Nikon NIS Element	Nikon, NY, USA	NA
Ingenuity	QIAGEN	NA
FlowJo	Tristar Inc, Stanford, CA, USA	NA

RESOURCE AVAILABILITY

Lead contact

Further information and requests for resources and reagents should be directed to and will be fulfilled by the Lead Contact, Chinnaswamy Jagannath (cjagannath@houstonmethodist.org).

Materials availability

Viral strains generated in this study will be made available upon request. A provisional patent application for BAdv85C5 has been filed by Purdue University and HMRI. Vaccines related to this study will be made available on request, but we may require a payment and/or a completed Materials Transfer Agreement if there is a potential for commercial application.

Data and code availability

The RNaseq dataset supporting the current study are available in NCBI database: NCBI Bioproject #PRJNA745965 (SRR15107864; SRR15107868; SRR15107867; SRR15107866; SRR15107869; SRR15107865; SRR15103113; SRR15103107; SRR15103114; SRR15103108; SRR15103112; SRR15103117; SRR15103116; SRR15103106; SRR15103109; SRR15103111; SRR15103115; SRR15103110). https://www.ncbi.nlm.nih.gov/sra/PRJNA745957

EXPERIMENTAL MODEL AND SUBJECT DETAILS

Mice

The age- and sex-matched (4-6 weeks old; M/F) C57BL/6 mice were purchased from Jackson laboratory, Bar Harbor, ME, USA, and housed under specific pathogen-free conditions in the animal facility of the University of Texas Health Sciences Center, Houston, where the experiments on mice were performed before the relocation of Dr. Jagannath to HMRI. Mouse in ABSL3 vivarium maintenance was in accordance with ethical and animal welfare committee protocols complying with the current PHS policy of USA.

Ethics statement

All animal experiments in this study were performed as per animal protocols verified and approved by the Institutional Biosafety Committee of University of Texas Health Science center, Houston (where part of this study was performed). The animal study was carried out in accordance with the US government PHS policy on Humane Care and Use of Laboratory Animals and the protocol for the same was approved by the UTHSC Animal Welfare Committee of under protocol number # AWC −16-0136. HMRI approval number for similar protocols is AUP-0620-0037.

Cell lines

The CD4 T cell hybridoma BB7 specific for the p25-epitope of Mtb Ag85B was a gift of Dr. Clifford V. Harding, Case Western Reserve University, OH. The F9A6 cell line is specific for a human epitope of Ag85B and donated by Dr. DH. Canaday, coauthor. Both were maintained as frozen stocks at −80°C and thawed cells culture in DMEM medium with β-ME.

Primary cells

CD14 beads (Miltenyi Biotec, USA) were used to purify primary human and mouse macrophages, which were then cultured in GM_CSF containing medium as described under methods.

METHOD DETAILS

Isolation and cultivation of primary mouse marophages and DCs (APCs)

The bone marrows from 4-6 week-old C57BL/6 mice (M/F) (Jackson research Labs, USA) were obtained by flushing both the femur and tibia. The pooled bone marrows from 2 mice at a time was centrifuged for five minutes at 1,000 rpm. The cells were washed two times in ACK lysing buffer (Fisher BW10-548E), followed by 1 mL of phosphate buffered saline (PBS), passed through a 36-gauge needle, and suspended in Iscove's Modified Dulbecco's Medium (IMDM) with 10% percent fetal bovine serum (FBS), 20 ng per milliliter granulocyte macrophage colony stimulating factor (GM-CSF) and antibiotics (penicillin and gentamicin). The cells were then plated into six-well plates and incubated at 37°C in a CO_2 incubator for one week, while spiking the wells with 2 mL of fresh medium every two days. After seven days, the wells are flushed and the pooled were transferred to a 50 mL tube. The cells were pelleted and resuspended in MACS buffer (PBS containing 0.5% FBS) at a volume of 400 μL per 10^8 cells. CD11c microbeads (Miltenyi 130-052-001) were then added to the cells, 100 μL per 10^8 cells. The cells were incubated at 4°C for 15 minutes, washed once in 1 mL of MACS buffer and resuspended into 500 μL of MACS buffer. During this time, the Miltenyi separation columns (Miltenyi 130-042-201) were prepared by rinsing once with 500 μL MACS buffer, one column per 10^8 cells and placed onto a magnetic holder. The cells are added to the columns and the pass through was collected. The macrophages and other cells pass through since they lack CD11c on their surface. The columns were washed three times with 500 μL MACS buffer and then removed from the magnetic holders. One mL of dissociation buffer was then plunged through the column, detaching the dendritic cells off the column. Wash off was repeated once. The flow-through macrophages were then run through another CD14 column repeating the procedure to purify macrophages. The cells (DCs and macrophages) were counted and plated into 24-well plates with 10^6 cells per well in IMDM supplemented with 10% FBS and GM-CSF, and allowed to differentiate for 4-7 days. The medium was replaced with a GM-CSF-free medium rested and cells were used for various assays.

APCs were used to conduct mycobacterial infection, antigen presentation assay, and confocal imaging studies. They were used as monolayers in 8-well slide cultures for antibody stains and in 24-well plates for antigen presentation assays (IL-2 assays) or Mtb CFU assays.

Bacterial strains and culture conditions

Log phase organisms of wild-type *M. tuberculosis* (Erdman strain) and BCG vaccine (ATCC; Pasteur strain) cultured in 7H9 broth for 7 days were frozen in aliquots. Before use, aliquots were thawed, washed three times in PBS (12,000 rpm; 15 mins), sonicated at 4 W using a sonication probe and dispersed suspension matched with McFarland #1 in turbidity (10^8 CFU/mL). A single cell colony forming unit (CFU) suspension of Mtb/BCG were made for infections by gentle centrifugation at 500 rpm for 5 min and the supernatants containing well dispersed organisms were used 10^7 CFU/mL.

Adenoviral vectors and culture conditions

BHH3 (bovine-human hybrid clone 3)[95] BHH2C (bovine-human hybrid clone 2C),[95] 293 (human embryonic kidney cells expressing HAdV E1 proteins),[96] and 293Cre (293 cells expressing Cre recombinase)[97] were propagated as monolayer cultures in minimum essential medium (MEM) (Life Technologies, Thermo Fisher Scientific, Waltham, MA) enriched with either 10% reconstituted fetal bovine serum or fetal calf serum (HyClone, Thermo Fisher Scientific) and gentamycin (50 μg/mL).

The production and characterization of BAdv (BAdV-3 E1 and E3 deleted empty vector),[80] and HAdv (HAdV-5 E1 and E3 deleted empty vector)[98] have been described previously. Gene constructs containing the immunogenic epitope Ag85B-p25 of Mtb without (85) or with AIP-C5 (85C5) were codon-optimized for rodent expression and synthesized commercially (GenScript Biotech Corporation, Piscataway, NJ). We adapted the technology of homologous recombination in bacteria[99] for the generation of BAdv vectors expressing the Ag85B-p25 epitope of Mtb without (BAdv85) or with AIP-C5 ($BAdv^{85C5}$) (Figure 1). For developing HAdv vectors

expressing the Ag85B-p25 epitope of Mtb without (HAdv85) or with AIP-C5 (HAdv^{85C5}) (Figure 1), we applied the technology of Cre recombinase-mediated homologous recombination.[100] The gene cassette in BAdv or HAdv vectors was under the control of the cytomegalovirus (CMV) immediate early promoter and the bovine growth hormone (BGH) polyadenylation signal. The presence of the foreign gene cassette in the vector was identified initially by restriction analysis followed by sequencing the region containing the gene cassette. The expression of the immunogenic epitope/s in vector-infected cells was confirmed by RT-PCR. BAdv, BAdv85 and BAdv^{85C5} vectors were grown and titrated in BHH3 cells as described.[24] Whereas HAdv, HAdv85 and HAdv^{85C5} vectors were replicated in 293 cells and titrated in BHH2C cells as described elsewhere.[101] All vectors were purified by cesium chloride density-gradient ultracentrifugation as described.[36]

Isolation and cultivation of primary human macrophages from peripheral blood samples

After obtaining informed consent, peripheral blood samples from healthy HLA-DR1 positive donors were obtained from Gulf Coast Regional Blood center. CD14 magnetic beads (Miltenyi, USA) were used to purify monocytes which were plated in 24 tissue culture plate wells for all experiments at 1x10^6 cells per well. CD14 bead purified monocytes were grown in Iscove's medium (IMDM) with 10% FBS and 10 ng/mL GM-CSF for 7 days and then plated in GM-CSF free medium for 24 hr before assay.

Infection of APCs with Adv vectors and vaccines

APCs were infected with BAdv or HAdv vectors (10^7 PFU per million APCs) followed by 4 hr incubation and washing three times with medium and incubation as indicated.

RNaseq analysis

Naive or BAdv/HAdv vector-infected MΦs or dendritic cells (2 X 10^6 cells per pellet; n = 2) were collected and mixed with Trizol buffer and snap frozen in liquid nitrogen. RNASseq analysis, data interpretation and pathway analysis were done by Novogene (USA). Additional bioinformatic analysis was done in-house. Targeted genes were validated using RT-PCR using probes as described below.

qPCR assay for gene expression in mouse bone marrow derived dendritic cells

Total RNA was extracted using RNAeasy mini kit (QIAGEN, Germany) from mouse bone marrow derived dendritic cells (DCs). RNA concentration and purity ratios (OD260/280, OD260/230) were measured using the NanoDrop ND-1000 spectrophotometer (Thermo Fisher Scientific, USA). cDNA synthesis was performed on a CFX96 Real-Time PCR System (Bio-Rad, USA) using the 2X OneStep qRT-PCR Mastermix Kit (Applied Biosystems, USA) according to manufacturer's instruction. Quantitative PCR (qPCR) was performed using SYBR green probe and gene specific primers (Table-primers). Threshold cycle numbers were transformed to $\Delta\Delta C_t$ values, and the results were expressed relative to the reference gene, β-actin and GAPDH. Gene expression data was performed using GraphPad Prism ver. 6.0 suite (GraphPad Software). Student's t test was used for means comparison between control or vaccine infected DCs. Significance was set at the 0.05 level.

Bronchoalveolar macrophages were aspirated from mice and pelleted in trizol for qPCR; Lungs were dissected, and equal amounts of fragments suspended in trizol. Primers for both DCs and mouse tissues are described in Figure S8.

Ex vivo Mtb Ag85B antigen presentation to CD4 T cells

The Ag85B epitope (241-256)-specific T cell hybridoma (BB7) was a kind gift from Drs. Cliff Harding (Case Western Reserve University, OH). The *ex vivo* antigen presentation assay has been described in detail by us, and the original method described by the Harding lab has been extensively used by us and others for *in vitro* antigen presentation by APCs (references cited in main text). Briefly, APCs infected with vaccines and vectors were washed 4 hr post-infection and overlaid with the BB7 CD4 T cell hybridoma which recognizes an Ag85B-p25 epitope in the context of mouse MHC-II (H2-d). IL-2 secreted from hybridoma T using a sandwich ELISA kit (eBiosciences). For human macrophages, the F9A6 cell line was used, which detects another Ag85B epitope in the context of human HLA-DR1.

siRNA knockdown of BAdv/HAdv vectors-infected APCs

The kits for various siRNAs (mixture of duplexes for Gal3, Gal8), were purchased from Origene as listed in the Key resources table. APCs were treated with siRNA and the scrambled control according to the manufacturers' instructions, and this was followed by an overlay with BB7 CD4 T cells and evaluation of antigen presentation.

Evaluation of virus containing endosomes and their colocalization with autophagolysosomes using antibodies and Cy3 labeled BAdv vector and vaccine in DCs

To visualize BAdv containing endosomes within DCs, BAdv vector and BAdv^{85C5} were labeled through covalent linking of the fluorescent dye, FluoroLink Cy3 (Amersham, Inc.), essentially as described by Leopold et al.[44] Briefly, BAdv stocks were adjusted to a concentration of 10*10 particles/mL and then mixed in a 1:9 ratio with Cy3 previously reconstituted in 0.1 M sodium carbonate, pH 9.3. After 30 min, the reaction mixture was transferred to a dialysis chamber (6,000-8,000 MW cutoff, Thermo Fisher) and dialyzed at 4°C for 24 hr against two changes of 10% glycerol, 50 mM Tris-HCl pH 7.5, 250 mM $MgCl_2$. Finally, the dialyzed mixture was then brought to 30% glycerol and stored at −20°C until use. For microscopy, mouse DCs were cultured on tissue culture chambered

slides or coverlips. Primary DCs were seeded at 10^4 cells per chamber and incubated at 37°C in a humidified incubator with 5% CO2, and used 24 hr after plating. DCs were infected using Cy3 labeled BAdv vector and $BAdv^{85C5}$ at 10^6 PFU per chamber for 4 hr. DCs were washed, fixed with 4% parafomaldehyde, permeabilized with a perm buffer (PBS with 0.05% tween 80. 0.01% SDS and 0.05% BSA) and labeled with LC3, LAMP1, Lgals-3 or Lgals-8 specific primary antibodies with an IgG isotype control overnight at 4°C. Alexa Fluor 488 (Thermo Fisher) tagged anti-IgG was used as secondary conjugate. Fluorescence microscopy was performed with an inverted Nikon N90 microscope equipped with 60-NA and a MetaView software which enables 3D-deconvolution of fluorescent images. Virus containing endosomes were determined counting individual puncta $\geq$ 200 nm labeling either red (C3 only) or labeling yellow after colocalization with specific antibodies. Noncolocalizing (red) or colocalzing (yelleow) endosome puncta (Figure 3) were counted inindividual DCs were averaged and repeated for 20 different DCs for duplicate chamabers. Data were expressed as percent endosomes labeling for antibodies and analyzed for signficance using t test and Graphpad prisim software. To avoid visual bias, pixel based colocalization was used.

Mouse vaccine experiments

The main mouse vaccine validation protocol is identical to the NIH mouse model that has beend described by us previously.[8] Age and sex matched mice (4-6 weeks) were tested naive or vaccinated with BCG via s.c. route to the hind legs of mice (confimed as 1×10^6 CFUs through plating on 7H11 agar). Intranasal vaccination with BAd and HAd viral vectors were then done after 7 days.Thirty days after prime boost vaccination, mice were aerosol challenged with ~100 CFU of virulent Mtb Erdman using a Glas-Col (Indiana, USA) aerosol apparatus. Four weeks (day 60) after challenge or at indicated times, organs were harvested for CFUs and cytometry. Significance of differences in the CFU counts was calculated using 2-way ANOVA. 5 mice per vaccine strain were used and three-four individual mice per time point for flow cytometry analysis. Two independent experiments were carried out, each with 5 mice per group and Figure 6C shows the combined CFU data. Challenge Mtb organsisms were differentiated from BCG vaccine by culturing organ homogenates in 7H11 agar containing Thiophene-2- carboxylic acid hydrazide (10 μg/mL), which inhibits BCG but not wild-type Mtb.

Post Mtb challenge flow cytometry for TRMs

Mice were sacrificed on day 60 post Mtb challenge to determine the numbers of lung resident TRMs. 5 mice per group were individually analyzed as follows. a) Lungs perfused with sterile phosphate-buffered saline were teased in buffer with 1 mg/mL collagenase and 1 mg/mL elastase (Sigma Biologicals, USA) to break down the fibrous tissue material. Single-cell suspensions from lungs and red cell lysed spleens were prepared in PBS with 10% FCS and 2 mM EDTA (Sigma-Aldrich) by straining through 40-μm cell strainer using a plunger of 5-mL syringe (BD Biosciences). Lung- and spleen-derived cells were stained for CD4 and CD8 T cells using antibodies to surface markers and intracellular cytokines as decsribed before.[8]

Flow cytometry analysis

Results were reported as absolute numbers of T cells per organs after performing an initial organ cell count using trypan blue and staining and acquiring a fixed number of cells. One million splenocytes or lung cells were stained using antibodies to CD3 (564380), CD8 (551162), CD4 (561025), CD62L (553150), CD44 (562464), CCR7 (12-1971-80), CD103 (562772), CD69 (740220), CD11a (740849), Live/Dead Fixable Aqua Dead Cell Stain Kit (L34957). All the antibodies were purchased by BD Biosciences. CCR7 antibody was purchased from eBiosciences and Live/Dead staining kit was purchased from Thermo Fisher Scientific. After fixation and storage at 4°C overnight, the cells were analyzed using a BD Fortessa flow cytometer. The FlowJo software program was used to analyze the data (Tree Star Inc., Stanford, CA).

For intracellular staining, cells were fixed and permeabilized according to manufacture instruction of using Fixation/Permeabilization Solution Kit with BD GolgiStop (554715: BD Biosciences) and stained for IFN-γ (564336: BD Biosciences) and IL-2 (560547: BD Biosciences). All staining antibodies were used at 1:200 or 1:300 or 1:500 dilution depending on the experiment. Sample acquisition was performed on a BD Fortessa flow cytometer using FACS Diva software followed by data analysis with FlowJo software.

Post vaccination and post Mtb challenge flow cytometry for TRMs

Mice were sacrificed on day 21 post vaccination and day 60 post Mtb challenge to determine the numbers of lung resident TRMs using CD103 and CD69 markers. 3 mice per group were individually analyzed.

Western blots: 'Wes Protein Simple' western assay / Wes analysis of proteins in lysates of DCs

For the analysis of protein levels in DCs, the quantitative Wes capillary immunoassay was used, in which the lysates were separated and detected using Wes separation capillary cartridge 12-230 kDa along with Wes Anti-Rabbit Detection Module (Simple Western system and Compass Software, Protein Simple). In brief, glass microcapillaries were loaded with stacking and separation matrices followed by sample loading. During capillary electrophoresis, proteins were separated by size and then immobilized to the capillary wall. Samples were loaded at 1 mg/mL dilution and the primary rabbit antibodies and GAPDH were used at 1:50 dilution. Data were analyzed with the Compass software (version 2.6.7). The area under the curve (AUC), which represents the signal intensity of the chemiluminescent reaction was analyzed for all the antibodies and βactin). Values given for protein expression were normalized to β-actin. Quantitation of protein levels (area under each peak; arbitrary units [A.U.]) were performed using the Compass software

(version 2.6.7). All the primary antibodies used for the Simple Western are listed in the Reagents Table. All the antibodies were purchased from Cell signaling or Novus biologicals.

QUANTIFICATION AND STATISTICAL ANALYSIS

All experiments were performed at least 2-3 times at different times. *Ex vivo* assays contained triplicate wells per group or combination. Statistical parameters including the definition of central value and spread (mean ± SD) and the exact number (n) of DCs or macrophages or mice per group are annotated in the corresponding figure legends. Statistical analysis was performed with GraphPad Prism version 8.04 for Windows (GraphPad) by using, unless otherwise stated, unpaired t tests with 95% confidence intervals. For statistical analysis of the microscopic quantification and intracellular survival of *M. tuberculosis,* the one-way ANOVA with Tukey's multiple comparisons test was applied. (* p value < 0.05; ** p value < 0.01; *** p value < 0.001; ns, not statistically significant). All CFU calculations in mouse experiments were done using 2-way ANOVA using Dunett's posttest.

Cell Reports Medicine, Volume *2*

Supplemental information

A recombinant bovine adenoviral mucosal vaccine expressing mycobacterial antigen-85B generates robust protection against tuberculosis in mice

Arshad Khan, Ekramy E. Sayedahmed, Vipul K. Singh, Abhishek Mishra, Stephanie Dorta-Estremera, Sita Nookala, David H. Canaday, Min Chen, Jin Wang, K. Jagannadha Sastry, Suresh K. Mittal, and Chinnaswamy Jagannath

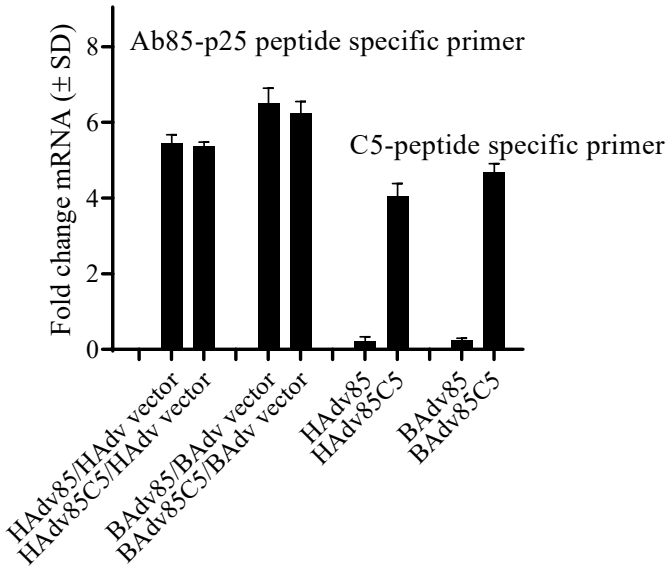

Supplemental Figure- 1a: qPCR validation of Antigen 85B derived p25 and CFP-10 derived C5 related to Fig.1. Primers shown in *Supplemental Fig.8.*

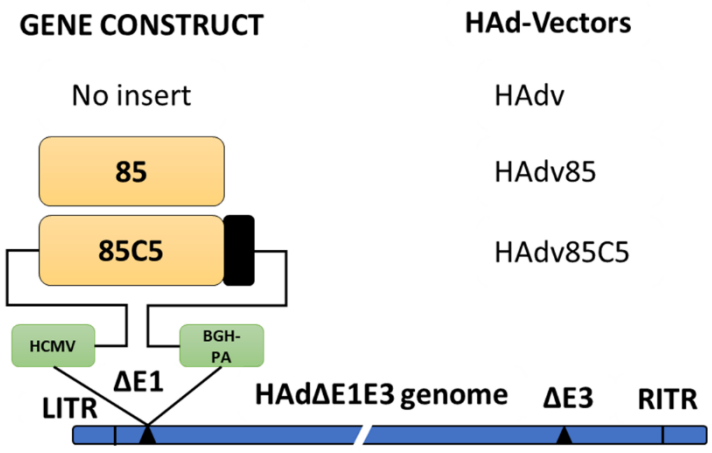

Supplemental Figure- 1b: Gene cassette of HAdv constructs related to Fig.1.

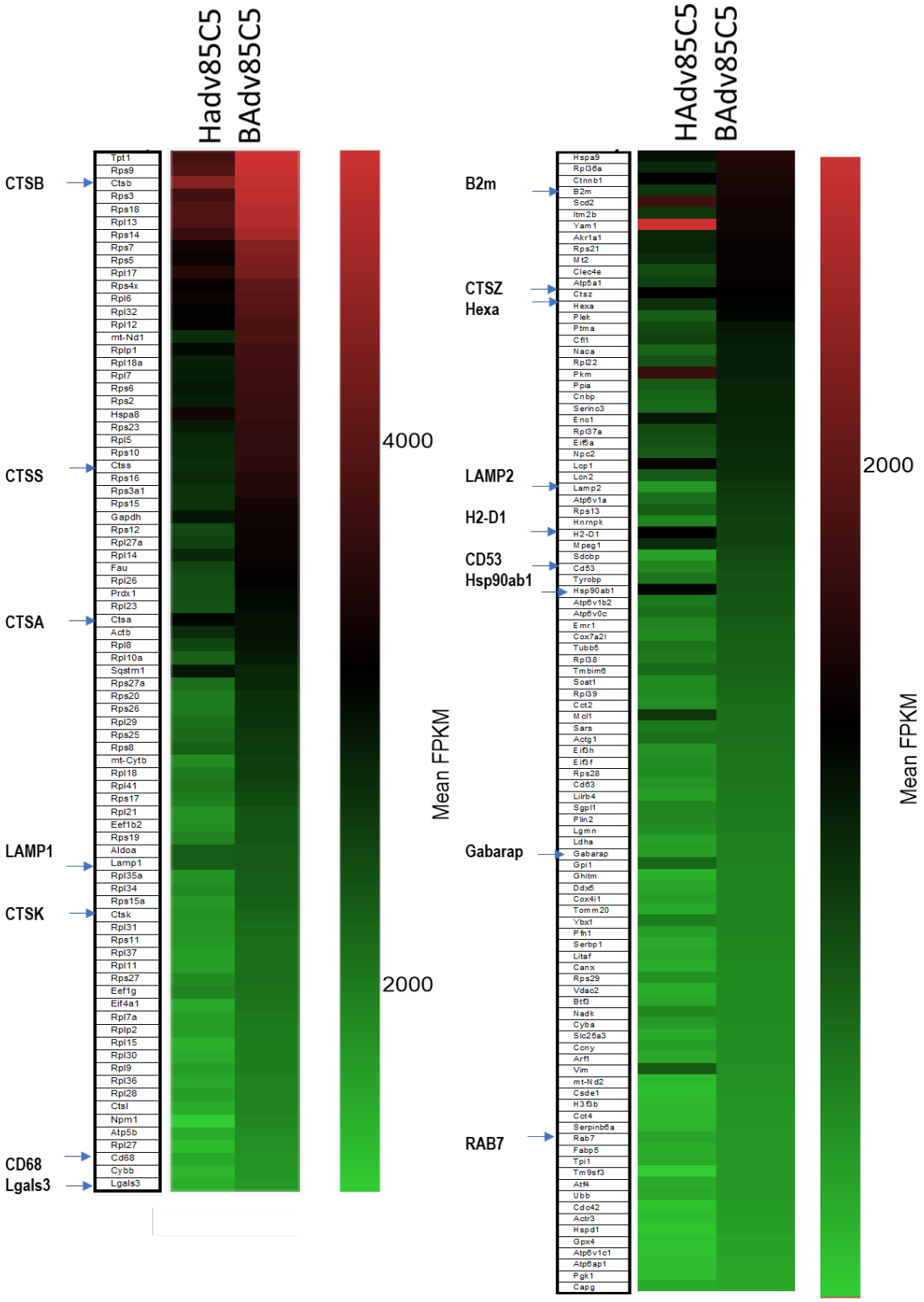

Supplemental Figure- 2: DEGs of HAdv^{85C5} in wt-DCs vs. BAdv^{85C5} related to Fig.2.

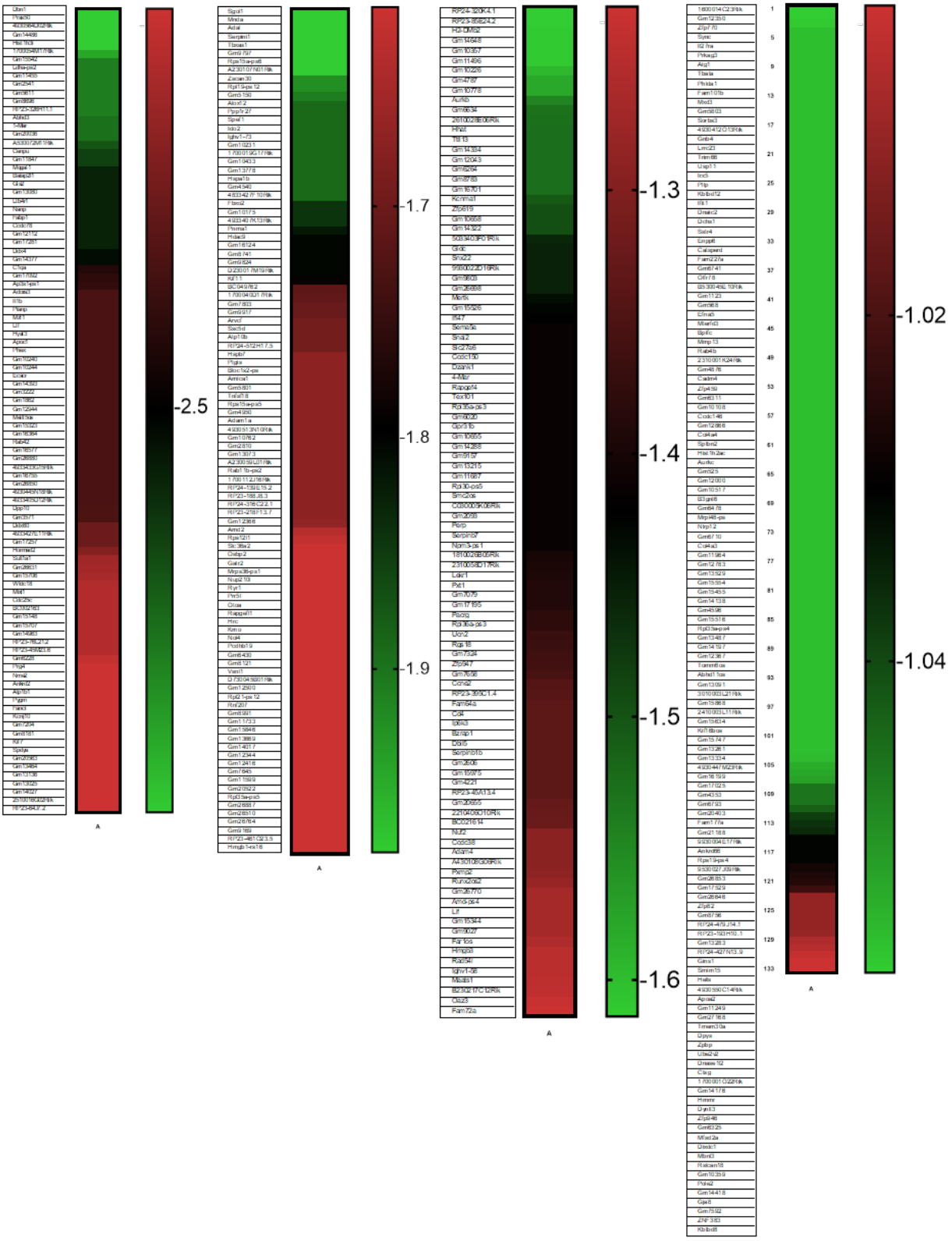

Supplemental Figure- 3: DEGs of BAdv^{85C5} in wt-DCs vs. BAdv^{85C5} in *ATG7*KODCs, related to Fig.2.

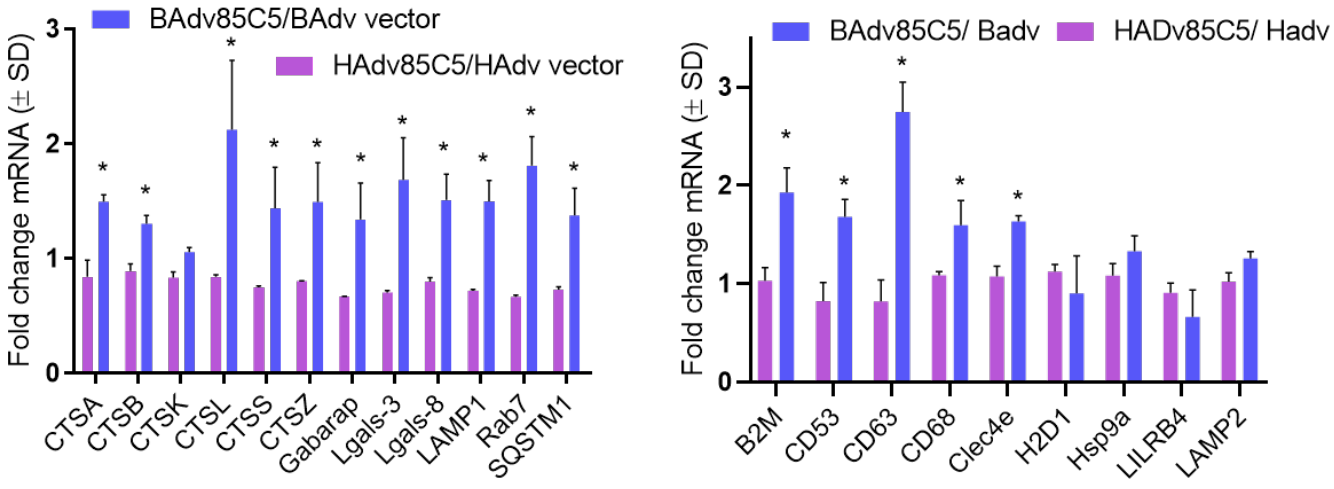

Supplemental Figure- 4: qPCR validation of genes in BAdv^{85C5} infected DCs vs. HAdv^{85C5} infected DCs, related to Figs. 2.

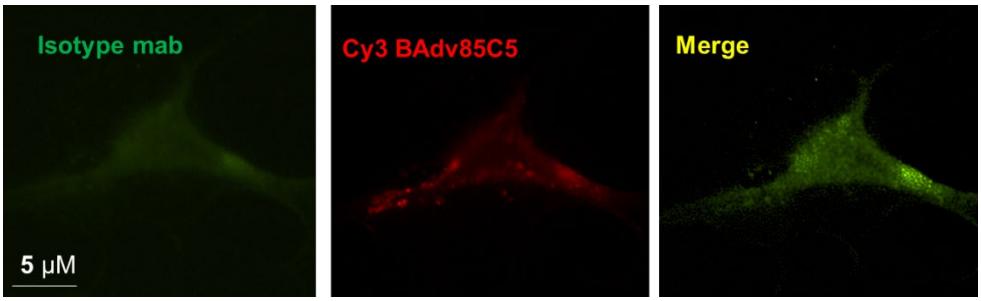

Supplemental Figure- 5: Isotype controls related to Fig.3.

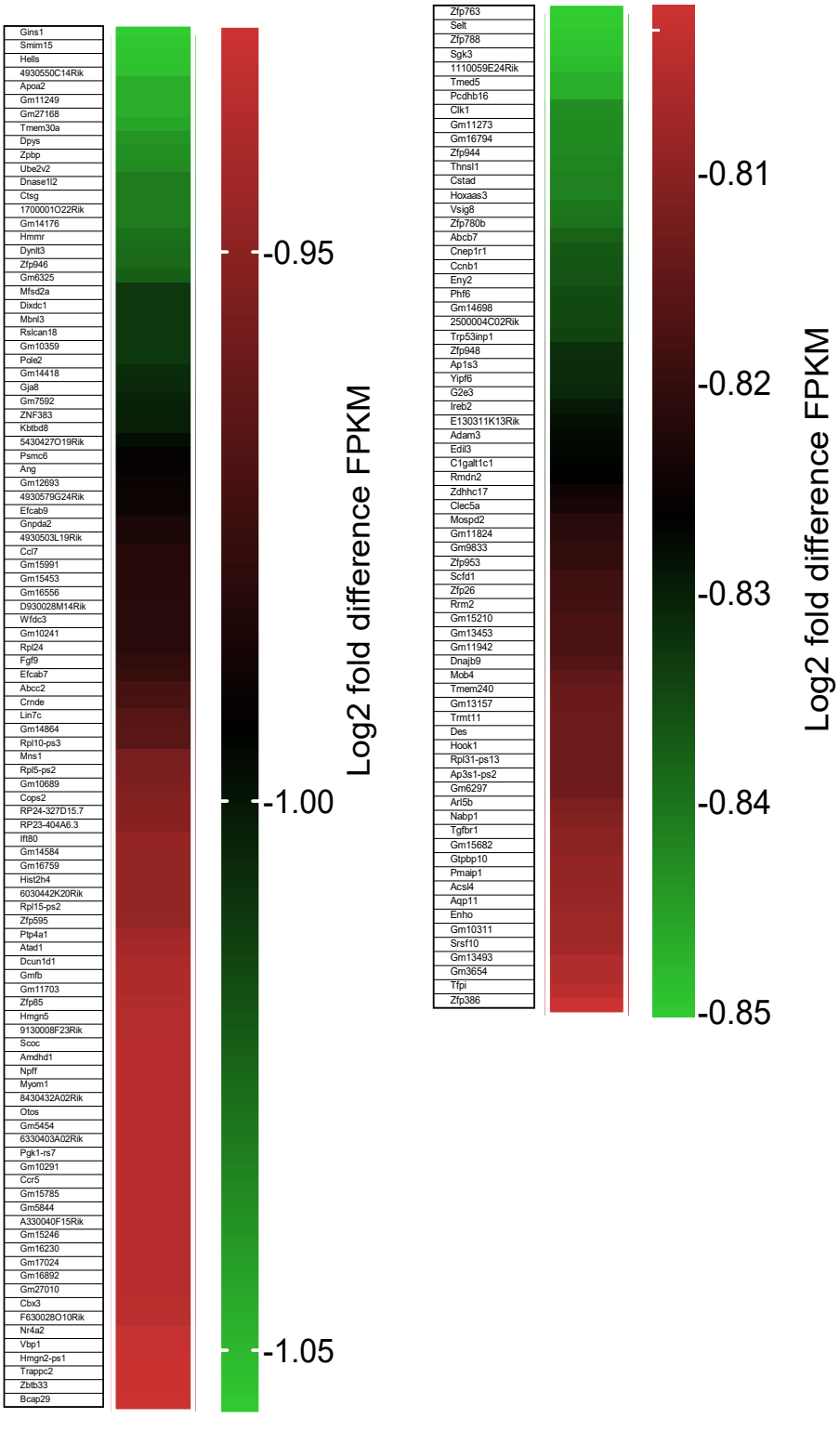

Supplemental Figure- 6: DEGs of BAdv^{85C5} in C57Bl/6 derived wt-macrophages compared to HAdv^{85C5}, related to Fig.2.

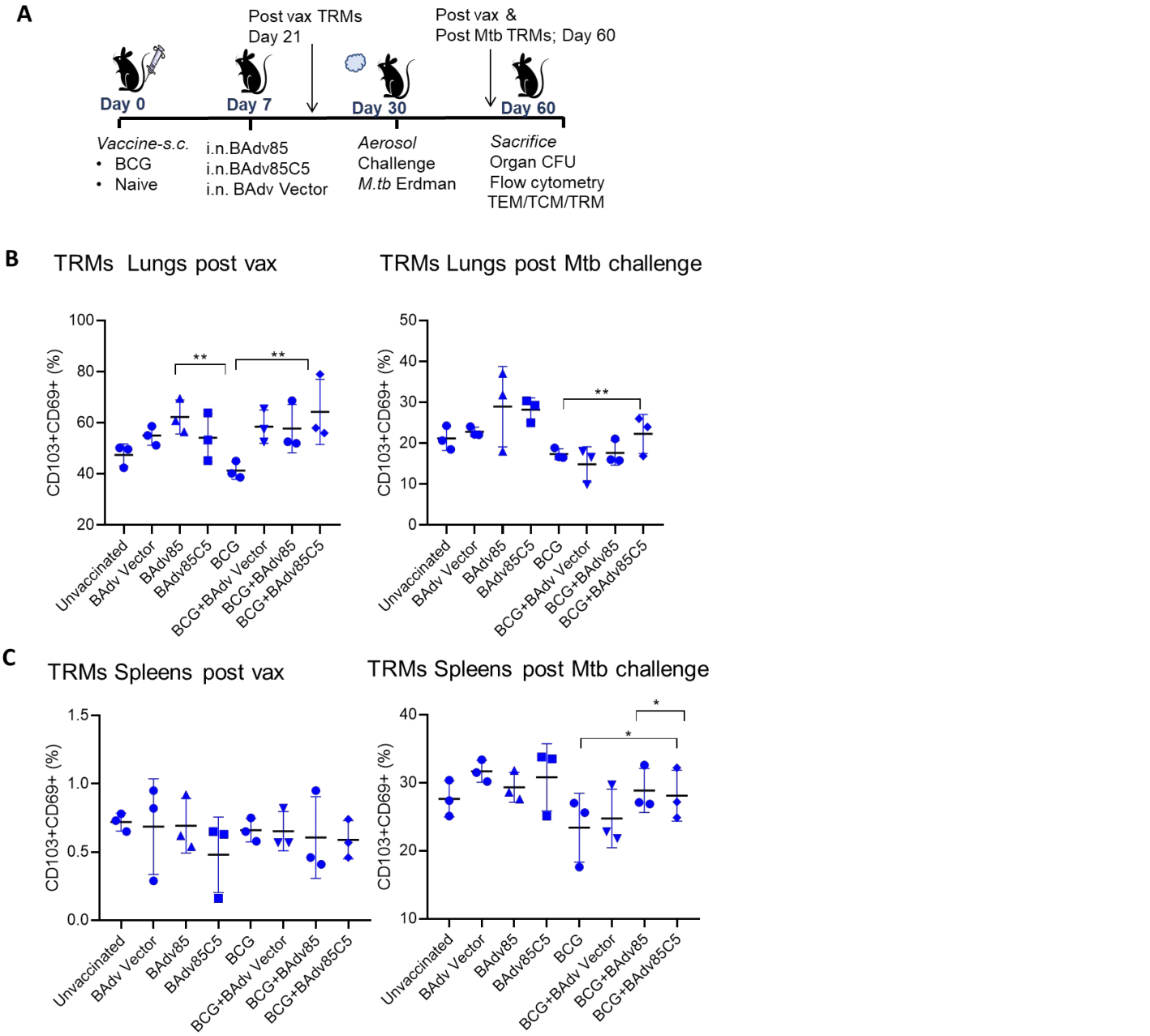

Supplemental Figure- 7: T_{RMs} ($CD4^{+}CD103^{+}CD69^{+}$) on day 21 for post vaccination and day 60 post Mtb challenge, related to *Fig.7.*

GENE	Forward primer 5'->3'	Reverse primer 5'->3'
Ag85b	GATATCGGATCCGCCACC	GCGGCCGCGATATC
Ag85bC5	GATATCGGATCCGCCACC	GCGGCCGCGATATC
β-Actin	CATTGCTGACAGGATGCAGAAGG	TGCTGGAAGGTGGACAGTGAGG
CTSA	TGTTCGGAAGGCTCTCCACATC	CACATCTCCGTTGTAGAGCAGG
CTSB	AGTCAACGTGGAGGTGTCTGCT	GTAGACTCCACCTGAAACCAGG
CTSK	AGCAGAACGGAGGCATTGACTC	CCCTCTGCATTTAGCTGCCTTTG
CTSL	GGAAAATGGAGGTCTGGACTCG	GTGTCATTAGCCACAGCGAACTC
CTSS	GCATAGAGGCAGACGCTTCCTA	CCACTGCTTCTTTCAGGGCATC
CTSZ	GTGTCAGCAACGATGGCATCGA	CCTTGTAGGTGCTGGTCACGAT
GABARAP	CAAAGAGGAGCATCCGTTCGAG	TTGTCCAGGTCTCCTATCCGAG
GAPDH	CATCACTGCCACCCAGAAGACTG	ATGCCAGTGAGCTTCCCGTTCAG
LGALS3	AACACGAAGCAGGACAATAACTGG	GCAGTAGGTGAGCATCGTTGAC
LGALS8	GAGGAGATCACCTACGACATGC	CGTACAGCAGAACATGCCTTCC
RAB7	GAGCGGACTTTCTGACCAAGGA	CAATCTGCACCTCTGTAGAAGGC
LAMP1	CCAGGCTTTCAAGGTGGACAGT	GGTAGGCAATGAGGACGATGAG
Sqstm1	GCTCTTCGGAAGTCAGCAAACC	GCAGTTTCCCGACTCCATCTGT

Fold change is calculated by using $2^{-\Delta\Delta Ct}$ method

Briefly,

ΔCt = Ct (gene of interest) – Ct (housekeeping gene)

$\Delta\Delta Ct$ = ΔCt (treated sample) – ΔCt (untreated sample)

Fold change = $2^{-\Delta\Delta Ct}$

Supplemental Figure- 8: qPCR primers used in this study; related to *Figs.5 and 6*.